

**SYNTHESIS AND CHARACTERIZATION OF bi/tri-METALLIC  
OXIDE THIN FILMS, AND THEIR APPLICATIONS IN DIRECT  
METHANOL FUEL CELLS FOR ELECTRO-OXIDATION OF  
METHANOL.**



**UJALA ZAFAR**

**Reg #: 00000278366**

**This work is submitted as a MS thesis in partial fulfillment of the requirement  
for the degree of  
(MS in Chemistry)**

**Supervisor's Name**

**Dr. Mudassir Iqbal**


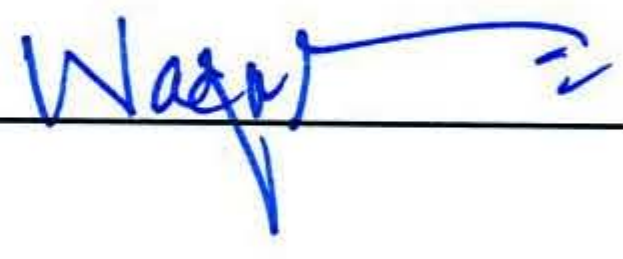
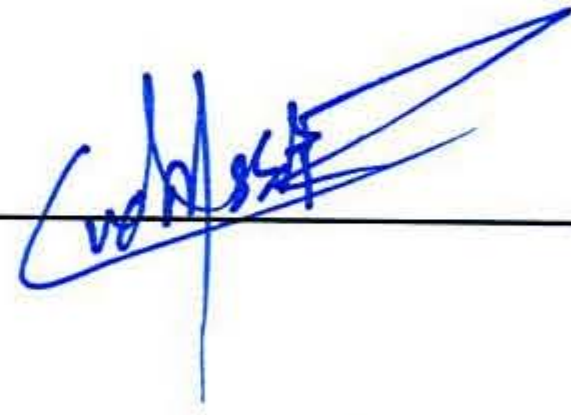
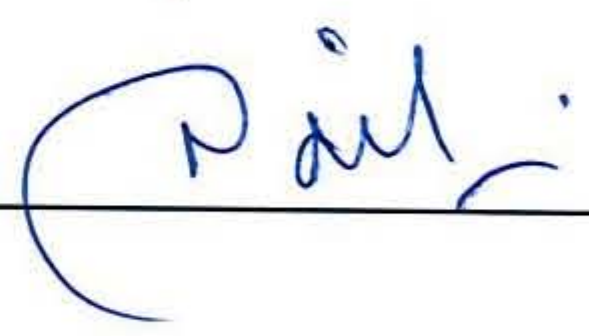
**Department of Chemistry**

**School of Natural Sciences (SNS) National University of Sciences and  
Technology (NUST), H-12, Islamabad, Pakistan.**



**National University of Sciences & Technology****MS THESIS WORK**

We hereby recommend that the dissertation prepared under our supervision by: Ujala Zafar, Regn No. 00000278366 Titled: Synthesis and Characterization of bi/tri metallic oxide thin films and their applications in Direct Methanol fuel cells for electrooxidation of Methanol be Accepted in partial fulfillment of the requirements for the award of **MS** degree.

**Examination Committee Members**1. Name: DR. AZHAR MAHMOODSignature: 2. Name: DR. SYED RIZWAN HUSSAINSignature: External Examiner: DR. WAQAR UN NISASignature: Supervisor's Name DR. MUDASSIR IQBALSignature: Co-Supervisor's Name DR. M. ADIL MANSOORSignature: 


Head of Department

18/10/21  
Date

**COUNTERSIGNED**Date: 20.10.2021


Dean/Principal



# Table of Contents

ACKNOWLEDGEMENTS .....	7
SUMMARY .....	8
1 CHAPTER 01.....	11
INTRODUCTION .....	11
1.1 Motivation and Background: .....	11
1.2 Fuel cells .....	12
Fuel cell system.....	13
Parts and working of Fuel cell .....	14
Classification of Fuel Cell Technology .....	16
1.3 Direct Methanol Fuel Cells.....	17
Mechanism of CH <sub>3</sub> OH oxidation in DMFCs in Basic media .....	19
DMFCs operate in two different ways according to the phase of fuel supplied. ....	23
Advantages of DMFCs.....	24
Disadvantages and challenges in the way of DMFCs.....	24
1.4 Electro-oxidation Catalysts for Methanol.....	26
1.5 Metal-oxide thin films .....	27
1.6 Thin layer deposition techniques .....	28
Dip Coating Method .....	30
AACVD METHOD .....	31
1.7 Characterization techniques.....	34
Scanning electron microscope (SEM) .....	34
X-Ray Diffraction Spectroscopy (XRD).....	35
Fourier Transform Infrared Spectroscopy (FT-IR) .....	37
1.8 Electrochemical techniques:.....	38
Cyclic voltammetry (CV).....	38
Electrochemical Impedance Spectroscopy (EIS).....	40
1.9 Objectives.....	42
2 CHAPTER 02.....	43
LITERATURE REVIEW.....	43
3 CHAPTER 03.....	51

<b>EXPERIMENTAL WORK .....</b>	<b>51</b>
<b>3.1 Materials .....</b>	<b>51</b>
<b>3.2 Instruments .....</b>	<b>51</b>
<b>3.3 Apparatus.....</b>	<b>51</b>
<b>3.4 Methodology .....</b>	<b>51</b>
Preparation of precursor’s solution .....	51
Synthesis of metal oxide composite (NiO-Mn <sub>2</sub> O <sub>3</sub> /FTO) thin films .....	52
Synthesis of metal oxide composite (NiO-(Mg-ZnO)/FTO) thin films .....	54
<b>3.5 Applications of prepared composite thin films in the electrochemical oxidation of Methanol .....</b>	<b>56</b>
<b>4 CHAPTER 04.....</b>	<b>58</b>
<b>RESULTS AND DISCUSSION .....</b>	<b>58</b>
<b>4.1 Characterization of (NiO-(Mg-ZnO)//FTO) and NiO- Mn<sub>2</sub>O<sub>3</sub> /FTO) thin films ...</b>	<b>58</b>
Energy Dispersive X-Ray Spectroscopy (EDX).....	58
Scanning Electron Microscopy (SEM) Analysis.....	59
X-Ray Diffraction (XRD) analysis.....	61
Raman Spectroscopic analysis .....	64
<b>4.2 Electrochemical oxidation of Methanol.....</b>	<b>66</b>
Cyclic Voltammetry (CV).....	66
Chronoamperometry (CA).....	74
Electrochemical Impedance Spectroscopy (EIS).....	76
<b>5 CHAPTER 05.....</b>	<b>78</b>
<b>CONCLUSION.....</b>	<b>78</b>
<b>6 CHAPTER 06.....</b>	<b>80</b>
<b>REFERENCES .....</b>	<b>80</b>

## List of Figures:

FIGURE 1: SOURCES OF GLOBAL ENERGY .....	12
FIGURE 2: DESCRIPTIVE REPRESENTATION OF FUEL CELL WORKING .....	16
FIGURE 3: COMPARISON OF DIFFERENT TYPES .....	17
FIGURE 4: ILLUSTRATIVE DIAGRAM OF DIRECT METHANOL FUEL CELL .....	18
FIGURE 5: ELECTROCHEMICAL REACTIONS INVOLVED DMFC.....	19
FIGURE 6: SCHEMATIC REPRESENTATION OF PATHS FOLLOWED FOR OXIDATION IN ALKALINE MEDIA .....	20
FIGURE 7: FOLLOWING STEPS ARE INVOLVED DURING OXIDATION.....	21
FIGURE 8: REPORTED ELECTRO-CATALYSTS FOR OXIDATION OF METHANOL .....	27
FIGURE 9: THIN FILM AND THICK FILM RULES.....	28
FIGURE 10: SCHEMATIC REPRESENTATION OF STEPS PERFORMED DURING DIP COATING METHOD. ....	31
FIGURE 11: SCHEMATIC DIAGRAM OF AACVD METHOD .....	33
FIGURE 12: DIFFERENT PARTS OF SCANNING ELECTRON MICROSCOPE .....	35
FIGURE 13: ILLUSTRATIVE DIAGRAM OF X-RAY DIFFRACTOMETER .....	37
FIGURE 14: ILLUSTRATIVE DIAGRAM OF FT-IR .....	38
FIGURE 15: SCHEMATIC-REPRESENTATION-OF-MEASUREMENT-SETUP-OF-CYCLIC-VOLTAMMETRY .....	39
FIGURE 16: CONVENTIONAL CYCLIC VOLTAMMOGRAM.....	40
FIGURE 17: ELECTROCHEMICAL IMPEDANCE SPECTROSCOPY (NYQUIST PLOT) .....	41
FIGURE 18: SCHEMATIC REPRESENTATION OF METAL OXIDE COMPOSITE THIN FILMS SYNTHESIS VIA DIP COATING METHOD. ....	53
FIGURE 19: SCHEMATIC REPRESENTATION OF SYNTHESIS OF NiO-(Mg-ZnO) FILMS ON FTO BY AACVD METHOD. ....	55
FIGURE 20: ELECTROCHEMICAL CELL CONSISTING OF THREE ELECTRODES .....	57
FIGURE 21: POTENTIOSTAT FOR ELECTROCHEMICAL STUDIEES.....	57
FIGURE 22: EDS SPECTRA OF NiO-(Mg-ZnO)/FTO THIN FILMS WITH TABLE 4 IN WHICH ATOMIC AND WEIGHT PERCENT OF ELEMENTS ARE MENTIONED. ....	58
FIGURE 23: EDS SPECTRA OF A) NiO B) Mn <sub>2</sub> O <sub>3</sub> C) NiO- Mn <sub>2</sub> O <sub>3</sub> .....	59
FIGURE 24: SEM IMAGES NiO-(Mg-ZnO)/FTO FILMS.....	60
FIGURE 25: SEM IMAGES OF A) NiO B) Mn <sub>2</sub> O <sub>3</sub> C) NiO- Mn <sub>2</sub> O <sub>3</sub> /FTO THIN FILMS. ....	61
FIGURE 26: X-RAY DIFFRACTION PATTERN OF NiO-(Mg-ZnO)/FTO THIN FILMS. ....	62
FIGURE 27: COMPARISON OF X-RAY DIFFRACTION PATTERN OF NiO-(Mg-ZnO)/FTO THIN FILMS SYNTHESIZED AT VARIOUS TEMPERATURES A) 400°C B)500°C C)550°C. ....	63
FIGURE 28:X-RAY DIFFRACTION PATTERN OF NiO/FTO, Mn <sub>2</sub> O <sub>3</sub> /FTO, NiO-Mn <sub>2</sub> O <sub>3</sub> /FTO THIN FILMS. ....	64
FIGURE 29: RAMAN SPECTRA OF NiO-(Mg-ZnO)/FTO THIN FILMS.....	65
FIGURE 30: COMPARISON OF RAMAN SPECTRA OF NiO, Mn <sub>2</sub> O <sub>3</sub> , NiO-Mn <sub>2</sub> O <sub>3</sub> /FTO THIN FILMS.....	66
FIGURE 31: CYCLIC VOLTAMMOGRAM OF NiO-Mn <sub>2</sub> O <sub>3</sub> /FTO FILMS IN 0.5M NaOH SOLUTION AT100 mV/s. A) IN ABSENCE OF METHANOL B) IN THE PRESENCE OF METHANOL .....	67
FIGURE 32: CYCLIC VOLTAMMOGRAM OF NiO-Mn <sub>2</sub> O <sub>3</sub> /FTO THIN FILMS IN 0.5M NaOH SOLUTION AT SCAN RATE OF 100mV/s. IN THE PRESENCE OF (0, 0.2, 0.4, 0.6, 0.8, 1, 1.2 AND 1.4M) METHANOL SOLUTION. ....	68
FIGURE 33: CYCLIC VOLTAMMOGRAM OF NiO, Mn <sub>2</sub> O <sub>3</sub> AND NiO-Mn <sub>2</sub> O <sub>3</sub> /FTO FILMS IN 0.5M NaOH AND 0.8M METHANOL SOLUTION AT 100 mV/s.....	70

**FIGURE 34: CYCLIC VOLTAMMOGRAM OF NiO-(Mg-ZnO)/FTO FILMS IN 0.5M NaOH SOLUTION AT 100 mV/s. A) IN ABSENCE OF METHANOL B) IN THE PRESENCE OF METHANOL ..... 71**

**FIGURE 35: CYCLIC VOLTAMMOGRAM OF NiO-(Mg-ZnO)/FTO THIN FILMS IN 0.5M NaOH SOLUTION AT SCAN RATE OF 100mV/s. IN THE PRESENCE OF (0, 0.2, 0.4, 0.6, 0.8, AND 1M) METHANOL SOLUTION. .... 72**

**FIGURE 36: COMPARISON OF CYCLIC VOLTAMMOGRAM OF NiO-(Mg-ZnO)/FTO FILMS PREPARED AT DIFFERENT TEMPERATURES A) 400°C B) 500°C C) 550°C FOR METHANOL OXIDATION IN 0.5M NaOH SOLUTION AT 100mV/s SCAN RATE. .... 74**

**FIGURE 37: CURRENT VS TIME PLOT OF NiO- Mn2O3/FTO FILMS AT APPLIED POTENTIAL OF 0.6V, IN THE PRESENCE OF 0.5M NaOH SOLUTION AND 0.8M METHANOL. .... 75**

**FIGURE 38: CHRONOAMPEROGRAM OF NiO-(Mg-ZnO)/FTO 550°C FILMS AT APPLIED POTENTIAL OF 0.6V, IN THE PRESENCE OF 0.5M NaOH AND 0.8M METHANOL. .... 76**

**FIGURE 39: NYQUIST PLOT OF Mn2O3, NiO, NiO-Mn2O3/FTO THIN FILMS IN THE PRESENCE (0.8M) OF METHANOL. .... 77**

**FIGURE 40: NYQUIST PLOT FOR NiO-(Mg-ZnO)/FTO 550°C THIN FILMS IN THE ABSENCE (0M) AND PRESENCE (0.8M) OF METHANOL. .... 77**

List of Tables:

<b>Table 1: Different techniques used for deposition.....</b>	<b>29</b>
<b>Table 2: Ceramic Oxide Thin Films Synthesized.....</b>	<b>54</b>
<b>Table 3: Metal oxide composite (NiO-(Mg-ZnO)/FTO) thin films at different temperatures.....</b>	<b>56</b>
<b>Table 4: Atomic and weight percent of elements are mentioned.....</b>	<b>59</b>
<b>Table 5: Current densities at 0.65V for various concentrations of Methanol .....</b>	<b>69</b>
<b>Table 6: Current densities at 0.65V for various concentrations of Methanol .....</b>	<b>73</b>

## ACKNOWLEDGEMENTS



All praises be to ALLAH, the Lord of the world, the Master of the Day After, who has given unlimited mercy to His creations which show Allah's love is spread around. He is the one who has love and teaches mankind of the power of His love; and from Allah's love, He sent the MESSENGER, Muhammad (peace be upon him) to guide mankind from wickedness to the truth of Islam. Thus, peace and salutation are uttered to beloved Prophet Muhammad SAW (peace upon him) who has brought mankind from cruelty and stupidity ages to peaceful and safety ages, Islam period.

Foremost, I would like to express my sincere gratitude to my supervisor **Dr. Mudassir Iqbal** for the continuous support of my MS study and research work, for his motivation and immense knowledge. I pay my deepest gratitude to my Co. Supervisor **Dr. Muhammad Adil Mansoor** for his guidance, patience, valuable cooperation for my research work, spiritual and moral support throughout the research journey. He played pivotal role in the accomplishment of this project. He always managed to guide me in the right research direction and never cared about working hours. I am thankful to him.

I pay my cardinal thanks to my GEC members **Dr. Azhar Mehmood** and **Dr. Syed Rizwan Hussain** for their assistance, insightful comments and kindness. I am greatly appreciative of academic and lab staff of **SNS** for being so helpful and friendly in taking care of my academic welfare.

I am thankful to **Mr. N. Hussain Khan, Mr. Kashif Ayub, Mr. Arsalan Umer, Dr. Waheed S. Khan** and National Institute for Biotechnology and Genetic Engineering (**NIBGE**), Faisalabad, Pakistan for facilitating me in the characterization of my materials.



I wanted to share how much blessed I am to have such a caring and compassionate family who I can always count on. I wish to thank my parents for their love and encouragement, without whom I would never have enjoyed so many opportunities. I am thankful to my ideal my father **Mr. Zafar Abbas Khan**, my beloved mother **Ms. Irshad**, and sisters (**Mahnoor Baloch, Sangat Balouch**).

A special acknowledgment goes to **Mr. Abrar Hussain and Ms. Mahnoor Baloch** for being there for me through thick and thin. Your positivity and kindness have made an unbearable time a little bit better. A special thanks to my friends **Fazeelat, Sarmad, Karishma, Rimsha and Nida** who never fail to make me smile. I appreciate you all for your love, support, and generosity.



***UJALA ZAFAR ABBAS KHAN***

## **SUMMARY**

Direct methanol fuel cells are emerging as a promising clean energy source. They have found applications from portable devices to transport sector. Still their practical applications are restricted due to slow kinetics and methanol crossover. Both anode and cathode electrocatalyst requires modifications. This work is related to synthesis of cheap, pollution free and efficient electrocatalyst for the oxidation of methanol. NiO-(Mg-ZnO)/FTO 550°C thin films are synthesized by AACVD method and NiO/FTO, Mn<sub>2</sub>O<sub>3</sub>/FTO, NiO-Mn<sub>2</sub>O<sub>3</sub>/FTO thin films were fabricated by Dip coating method. Nickel (II) acetate dihydrate [Ni (CH<sub>3</sub>COO)<sub>2</sub>.2H<sub>2</sub>O], Manganese (II) acetate tetrahydrate [Mn(CH<sub>3</sub>COO)<sub>2</sub>.4H<sub>2</sub>O], Zn(II) acetate dihydrate [Zn(CH<sub>3</sub>COO)<sub>2</sub>.2H<sub>2</sub>O], and Magnesium(II) acetate tetrahydrate [Mg(CH<sub>3</sub>COO)<sub>2</sub>.4H<sub>2</sub>O] were selected as precursors as they are easy to dissolve in solvents like, ethanol and methanol. Different techniques were used for the characterization of synthesized thin films. Elemental composition was confirmed by EDS analysis and SEM analysis showed that films are uniform and porous. X-ray diffraction and Raman analysis gave information about crystal structure, phase, crystallinity and confirmed the formation of impurity free ceramic thin films.

Electrocatalytic performance of synthesized films for electro-oxidation of methanol was investigated by use of a three-electrode system based potentiostat in 0.5M electrolyte solution of NaOH. The electrochemical studies were completed in the potential range of (-0.5 to 2V) and scan rate of 100mV/s by using various electrochemical techniques such as cyclic voltammetry (CV), electrochemical impedance spectroscopy (EIS) and chronoamperometry (CA). NiO-(Mg –ZnO) /FTO thin films fabricated by AACVD method at 550 °C showed better electrochemical activity with current density of 3.2mA/cm<sup>2</sup> vs 0.65 V and maximum value 20.9 mA/ cm<sup>2</sup> in the presence of 1M methanol. The NiO- Mn<sub>2</sub>O<sub>3</sub> /FTO thin films synthesized by Dip coating method showed electrochemical activity with current density 2.35mA/cm<sup>2</sup> vs 0.65 V and maximum of 25.8 mA/ cm<sup>2</sup> in 1.4M methanol. It is the synergistic effect between the metal oxides which is responsible for improved catalytic activity of NiO-(Mg –ZnO) /FTO and NiO- Mn<sub>2</sub>O<sub>3</sub> /FTO thin films. The change in scan rate has direct effect on current densities as transfer of electrons increases or decreases according to change. Chronoamperometric analysis was performed to measure the stability of films. The NiO-(Mg –ZnO) /FTO and NiO- Mn<sub>2</sub>O<sub>3</sub> /FTO thin films showed stabilities of 99% and 86% for 2000s. Small decay in current densities is due to decrease in concentration of

methanol with passage of time and formation of intermediates like  $(\text{CH}_3\text{OH})_{\text{ad}}$ ,  $\text{CO}_{\text{ad}}$ , and  $\text{CHO}_{\text{ad}}$  during the electrooxidation of Methanol. EIS studies were also conducted, and they revealed that in the presence of methanol the charge transfer resistance has decreased. The  $R_{\text{ct}}$  value for NiO-(Mg -ZnO) /FTO thin films is 571kohm. For NiO-  $\text{Mn}_2\text{O}_3$  /FTO thin films  $R_{\text{ct}}$  value is  $71\Omega$  which is smaller than the  $R_{\text{ct}}$  values for pure NiO and  $\text{Mn}_2\text{O}_3$  films  $349\Omega$ ,  $517\Omega$ , respectively. The as synthesized ceramic films showed improved catalytic activity, high stability towards oxidation of methanol in basic media in terms of both onset potential and current density. They are proved good candidate to be used as anode catalyst for electro-oxidation of Methanol in Direct Methanol Fuel Cells.

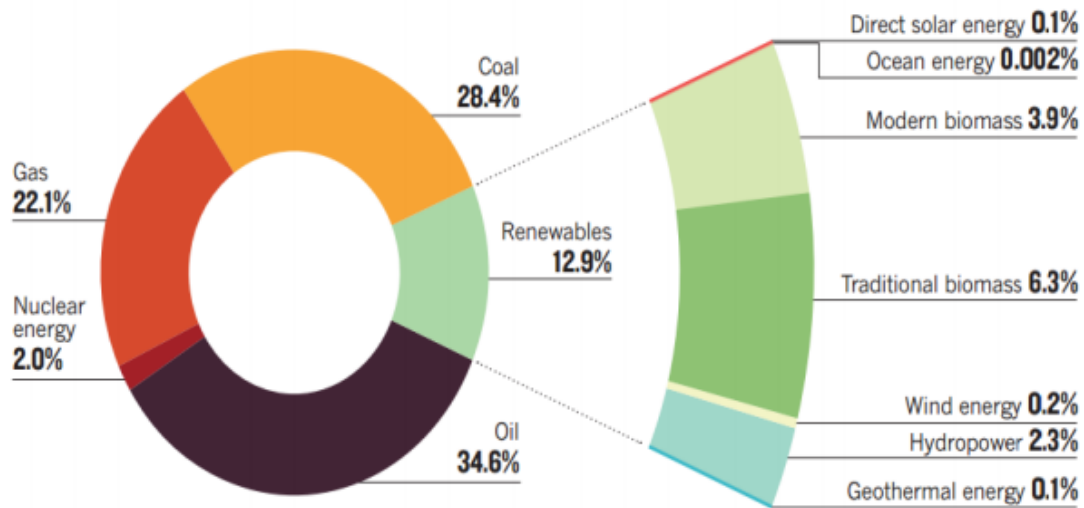
# 1 CHAPTER 01

## INTRODUCTION

### **1.1 Motivation and Background:**

Today, when the global population is growing rapidly, the economic development and requirement for a large amount of energy are going parallel<sup>1</sup>. Presently, the demand for global energy production is 13 terawatts and most probably it will reach 30 terawatts by 2050<sup>2</sup>. It is evident that the major source of energy for industry and transportation is a fossil fuel. This utilization of fossil fuels will further enhance in the coming decades. Where fossil fuel is distributed unevenly in the land and is continuously depleting<sup>3-5</sup>. Moreover, the massive use of fossil fuels is responsible for climate change as they are increasing the level of SO<sub>x</sub>, NO<sub>x</sub>, CO<sub>2</sub>, and CO in the atmosphere. The contaminated environment is not only increasing global warming but also several lethal diseases such as skin cancer and lung cancer have emerged over time. <sup>6-9</sup>

Global energy security and sustainability can be achieved by de-carbonization of energy by utilizing alternative renewable energy<sup>10,11</sup>. Although Pakistan is blessed with renewable resources but still, its energy production sector is dependent on non-renewable resources. As the population is growing rapidly the annual rise in energy demand is estimated to be 3%. The development of a country either it is social or economic is directly related to the energy supply of that country. It is the necessity of time to overcome the energy crisis in Pakistan by developing new policies and strategies to produce energy from renewable resources. The traditional system for energy production should be upgraded according to modern techniques to meet energy requirements. <sup>12,13</sup>



**Figure 1: Sources of Global Energy**

The contribution of different sources to our global energy showing that fossil fuels account for 81% and non-fossil fuel sources 19% of total energy. Data from International Energy Agency (iea.org)

In this scenario, the technology labeled as Fuel cells are emerging as one of the promising renewable resources of energy as compared to combustion energy sources. Fuel cells are replacing traditional resources of energy as they have found applications in every field of life from low power portable devices to electricity production units. They are more efficient, environment friendly, produces no noise during their operations and water is the only byproduct. Still, there are many technical challenges in making fuel cells technology acceptable in this modern age of technology as its output voltage is low and current dependent.<sup>14</sup>

## 1.2 Fuel cells

An electrochemical device in which chemical energy of fuel (i.e Hydrogen or hydrocarbon) is directly converted into electrical energy is called a Fuel cell. This single step energy conversion process has many advantages over multi-step processes occurring in conventional combustion-based technologies. During the process of combustion, harmful gases are emitted which are changing the climate, depleting the ozone layer, and causes acid rain which has dangerous effects

on plants, animals, and humans. The fuel cells are pollution free, efficient, simple, and renewable resources. The efficiency of fuel cells in converting chemical energy to electrical energy is estimated as 60% which is higher than combustion engines. In the hydrogen fuel cells, the only by-product is water along with heat and electricity, so they have no contribution to polluting the environment. They create no noise and many of their parts are stationary. Some features are common between fuel cells and batteries as:

- Both consists of an anode, cathode, and electrolyte
- In both Energy, conversion occurs by an electrochemical reaction
- Individual DC cells are arranged in series to attain high voltage and power

But in many aspects fuel cell technology is distinct from rechargeable batteries. Fuel cells require direct supply of hydrocarbon/hydrogen fuel as an energy source, their anode and cathode are gases (H<sub>2</sub>& O<sub>2</sub>) not metals, energy is only generated not stored in them. Fuel cells are stable as they are not consumed during chemical to electrical conversion of energy by electrochemical reaction.<sup>15-17</sup> That's why Fuel cells are becoming popular in each sector such as military, space, industrial, portable, transportation, residential, and trading. They have both stationary and mobile applications.<sup>18-20</sup>

### **Fuel cell system**

For the first time about 150 years ago William Grove gave the idea of fuel cells. The purpose behind the idea was to investigate the reverse process of electrolysis. In 1932 they were successfully implemented for the first time by Francis Bacon. The fuel cells generated by NASA are still in use as an electric generator in space shuttles. Now other industries are taking much interest and investing a lot in fuel cell technology as they are emerging as a clean and uninterrupted source of energy.<sup>21,22</sup>

A complete fuel cell system has six subsystems.

#### **1. An air supply system**

This system performs the function of filtration, pressurization, humidification, and preheating of the air supply according to requirements.



## **2. Fuel processing system**

The functioning of this system is dependent on application type. For mobile applications simple fuels hydrogen and methanol are used and transferred directly to stacks. In case of stationary applications, hydrocarbons are used, and they require conversion to hydrogen before transfer to fuel cell stack.

Reformers are used for the conversion of hydrocarbons or alcohols to a mixture of hydrogen, carbon, and oxygen.

## **3. Thermal management system**

The amount of chemical energy that is converted to thermal energy is taken up by a thermal management system which uses it for preheating the fuel or air. It can also be transferred externally for performing cogeneration applications.

## **4. Power management system**

The system performs the function of regulating stack voltage according to current load, protects the stack from damage by stopping short time power demands, and manages the output voltage following the requirement of the application.

## **5. Fuel cell stack system**

It consists of many cells connected in series. Air and fuel are supplied to each cell and DC is generated at a voltage of  $<1$ . The voltage range for the stack system is dependent on the number of series-connected cells. The stack voltage and current load are inversely related to each other.

## **6. Water management system**

This system requires water for humidification of fuel or air, and during the reforming step. Water is provided either by connecting to an external source or is recovered from exhaust generated from the stack.

These systems are constructed according to the applications required and the type of Fuel cell's stack.<sup>20</sup>

## **Parts and working of Fuel cell**

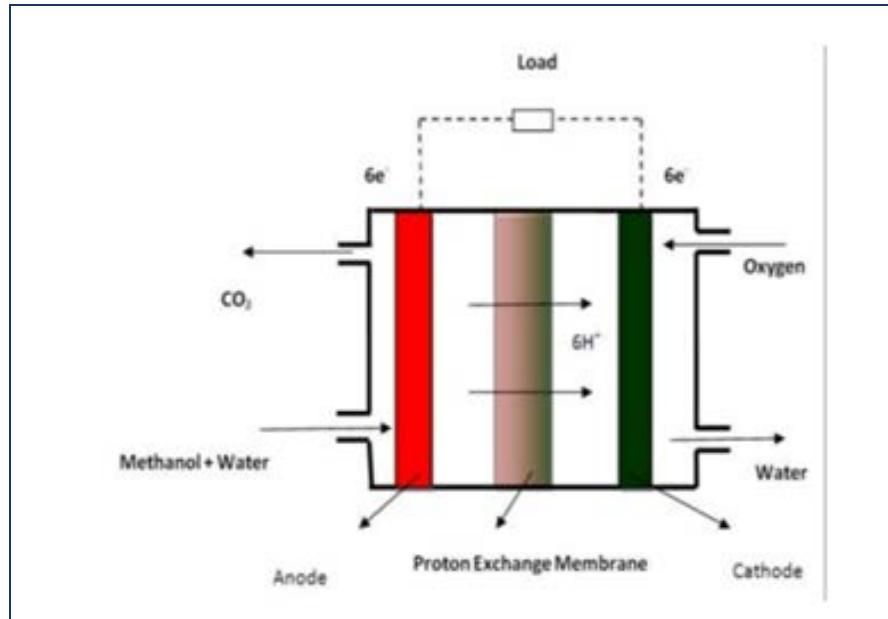
Working of the fuel cells is just like batteries, but they need not be recharged. They require an external and continuous source of fuel for the production of heat and electricity.

Their major parts are:

- Anode – fuel is oxidized at the (-ve) electrode
- Cathode – reduction of O<sub>2</sub> occurs at the (+ve) electrode
- Electrolyte – it transfers the ions and electrons between electrodes
- Collector plates – are used to develop connections between electrodes and external load.  
They also develop flow channels for the transmission of reactants and products.

In a hydrogen fuel cell, the hydrogen is supplied to the negative electrode, where a molecule of hydrogen is ionized to electrons and protons by a catalyst present on the anode. They will reach the cathode by following different paths. The electricity is generated by the passage of electrons from an external circuit. The protons will reach the cathode through the electrolyte. Heat and water are the byproducts that are formed as a result of the combination of protons with electrons and oxygen present at the cathode. The process of electric current production will continue in the external circuit if there is a continuous supply of reactants to the electrodes and the electrolyte is not affected by chemical reaction.

If alternating current is required, then a device called inverter is used for the conversion of DC output to AC current.<sup>20</sup>

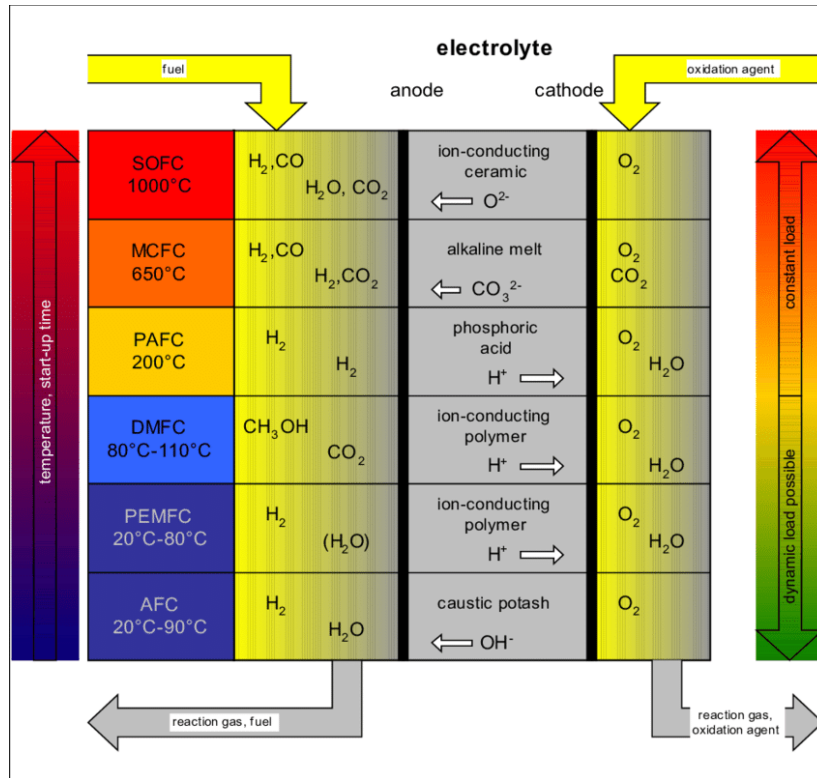


**Figure 2: Descriptive representation of Fuel cell working**

### **Classification of Fuel Cell Technology**

Some important factors such as electrolyte type, temperature, and source of fuel, which in turn affects their applications are considered during their classification. The chemical activity and lifespan of fuel cells are mainly affected by operating temperature. Thus, operating temperature range is specified for each type. Fuel cells are categorized into following major types.<sup>23,24</sup>

1. Polymer electrolyte membrane fuel cells
2. Direct methanol fuel cells
3. Alkaline fuel cells
4. Phosphoric acid fuel cells
5. Molten carbonate fuel cells (High temperature)
6. Solid oxide fuel cells (High temperature)
7. Reversible Fuel Cells

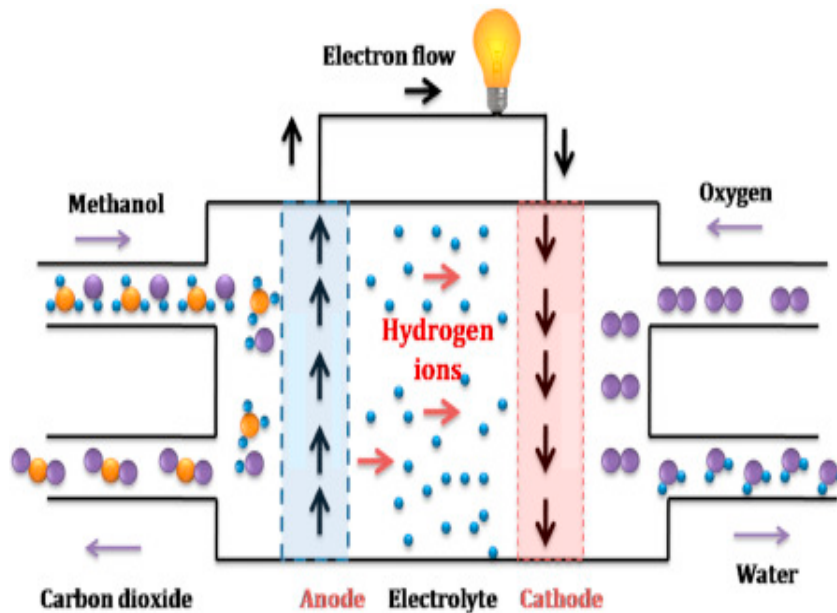


**Figure 3: Comparison of Different Types**

### 1.3 Direct Methanol Fuel Cells

Direct methanol fuel cells (DMFC) are emerging as promising energy source. The use of liquid reactant differentiating them from other types. The electric current is generated when Methanol (liquid fuel) is supplied to the anode and where it undergoes direct conversion process. They are sub-category of polymer electrolyte membrane fuel cells, but the only difference is the use of methanol as an alternative of H<sub>2</sub>, as a result, the power density has reduced to one-tenth as compared to (PEMFC). The researchers and developers are taking much interest in DMFC technology for utilizing them in portable devices and the transport sector because of their high energy densities, no emission of poisonous gases, compact structure, low operational temperature, and easy handling of methanol as fuel. In DMFC the role of the reformer is eliminated because the methanol is directly supplied to the anode where it is oxidized. Methanol is selected as fuel because it is inexpensive, less toxic, cartridges used for methanol are easy to handle, and energy capacity is higher than liquid hydrogen. It can be obtained from biomass or natural gas by using different methods<sup>25-27</sup>

A typical DMFC has a polymer electrolyte membrane assembly and two electrode plates. This membrane is responsible for the selective transmission of protons and electrons from one electrode to another. Methanol plus water is supplied directly to the reactor and a multi-step methanol oxidation reaction occurs at anode resulting in the generation of electrons, protons, heat, and CO<sub>2</sub>. Protons pass through membrane electrolyte and reaches to negatively charged electrode. At the cathode, the protons combine with oxygen and electrons results in the formation of water and heat the reaction is referred to as oxygen reduction reaction (ORR). The electrons produced from anodic reaction moves to an external circuit for the generation of electricity.



**Figure 4: Illustrative Diagram of Direct Methanol Fuel Cell**

**Following electrochemical reactions are involved in DMFC**

Reaction at anode (Oxidation): 0.03 V



Reaction at cathode (Reduction): 1.22 V



Overall reaction: 1.19 V



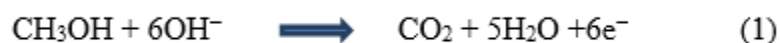
28

**Figure 5: Electrochemical Reactions involved DMFC**

**Mechanism of CH<sub>3</sub>OH oxidation in DMFCs in Basic media**

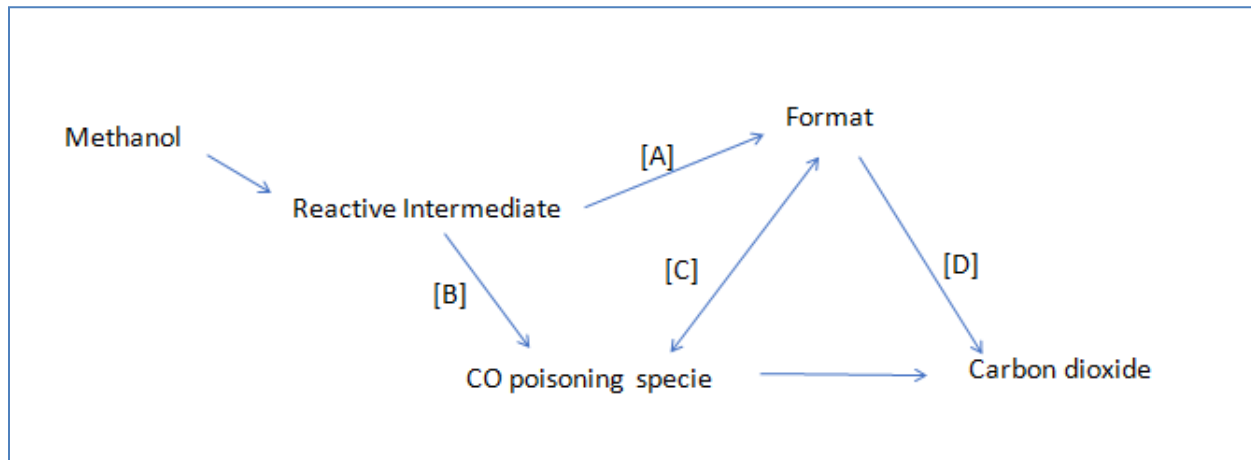
Higher efficiencies and electro-activity for CH<sub>3</sub>OH oxidation could be achieved in basic media as compared to acidic. The demand for alkaline fuel cell technology is rising as they are simple, cheap, efficient, with improved kinetics for oxygen reduction, and allows a range of electrolytes to be used. In DMFCs use of alkaline electrolytes has many advantages such as the required amount of catalyst which is to be loaded has been reduced and permits the use of low priced non-noble metals( Ni, Fe(III), Al) as electrocatalyst.<sup>29-31</sup>

In an alkaline medium:



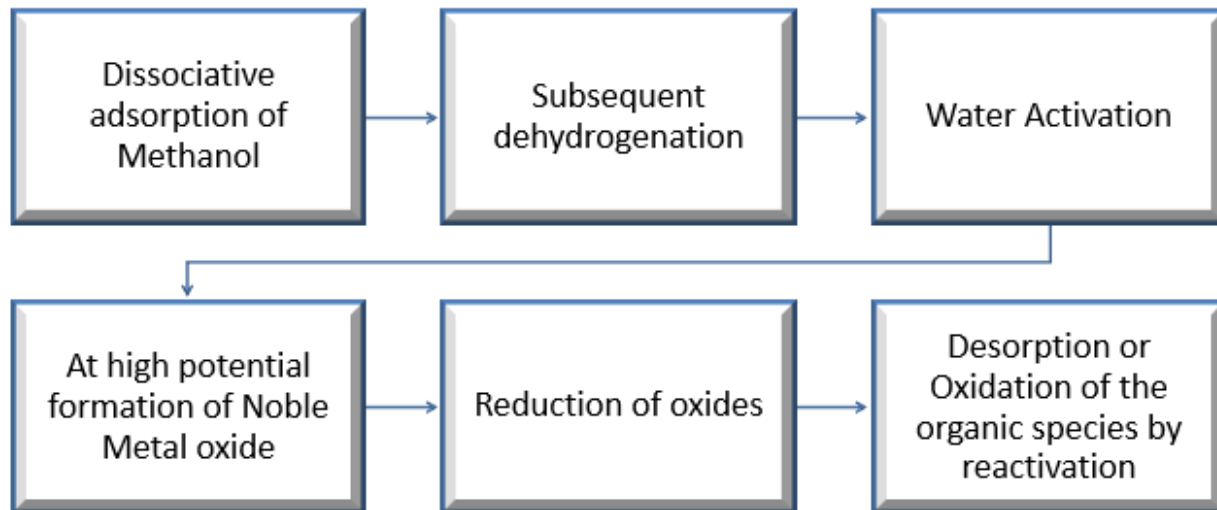


The electro-oxidation of methanol is a very complex process that involves the transfer of six electrons and many organic species are produced as intermediates. Following paths are adopted in the course of electro-oxidation of Methanol under basic conditions. (Figure 6)



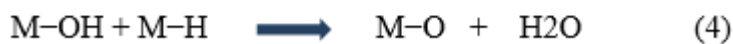
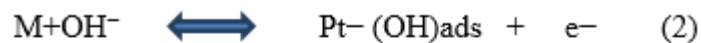
**Figure 6: Schematic representation of paths followed for oxidation in Alkaline media**

Major products of the reaction are Formate and CO<sub>2</sub> along with CO as poisoning substances in alkaline medium. The temperature and potential are the main factors that decide which path will be followed and what will be products. The steps involved in the oxidation process are listed in Figure 7.



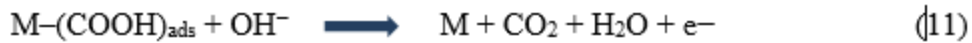
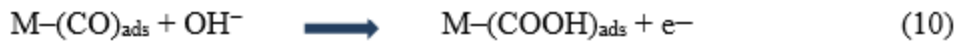
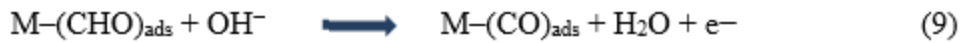
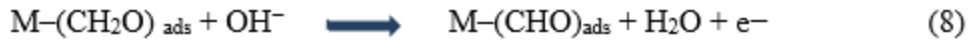
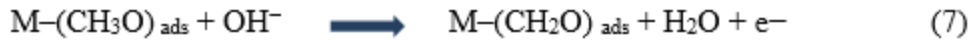
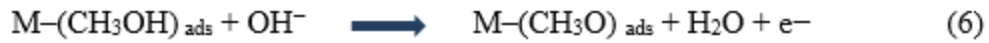
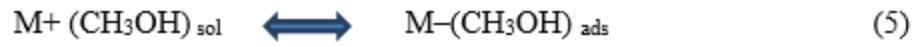
**Figure 7: Following steps are involved during oxidation**

When OH<sup>-</sup> ions are adsorbed on the surface of electrode they initiate the synthesis of oxides and hydroxides. At electrode-electrolyte interface following electrochemical reactions are occurring:



- **Dissociative adsorption of methanol**

At the anode surface, multiple steps that are involved in the chemisorption of methanol are listed below:



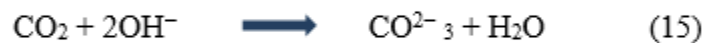
Where M stands for Pt-Pd

When a sufficient amount of alkali is present then the  $M - (\text{CHO})_{\text{ads}}$  and  $M - (\text{CO})_{\text{ads}}$  species will undergo direct oxidation reaction to produce  $\text{CO}_2$  by following steps (12) and (13)



The response rate is determined by the binding power of the (CHO) ads above. Complete removal of CO is possible only with high efficiency as it is highly integrated into the electrode surface.

Following are the steps for the reduction of oxygen at the cathode:



Overall reaction:



The problem with an alkaline fuel cell is the formation of carbonate and bicarbonates which decreases the electrolyte concentration that leads to lowering the performance of the cell. Improvements in the functions of alkaline fuel cells can be achieved with

- Electrolyte recycling
- Continuous removal of carbon dioxide to prevent the formation of carbonate

Better efficacy and inhibition of methanol flow to cathode have been achieved through the formation of a membrane-free laminar flow cell (LFFC) and an alkaline- anion exchange membrane (AAEM) application in AFC.<sup>32-34</sup>

**DMFCs operate in two different ways according to the phase of fuel supplied.**

❖ **Active DMFCs:**

They require auxiliary gears like blowers, pumps, and fans for the supply and removal of air, water, and methanol. They cannot be used for portable applications as they cover large volumes; handling is difficult and much expensive. More reliable and convenient to use for controlling the operation conditions like temperature, flow rate, and concentration of methanol.

❖ **Passive DMFCs:**

Their construction is easy as no external device is required. The oxygen and methanol are transferred passively by processes such as gravitation, diffusion, capillary forces, and natural convection. They require lower current density for their operation thus reducing the issues of water and heat management. They are suitable for portable applications as their size is small. They have a compact and simple design, more reliable, cheap, and give high energy density values.<sup>35,36</sup>

They are often driven by low current energy leading to reduced cooling load, lower water management issues, lower heat production, and lower fuel delivery rates.

## **Advantages of DMFCs**

- Methanol is considered as the best choice to use as fuel. As the complete oxidation of one molecule of methanol generates six protons and electrons.
- They are not posing any problem to the environment as no toxic gases are released. Only CO<sub>2</sub> (a greenhouse gas) is produced as a by-product.
- DMFCs are more efficient for stationary applications as compared to traditional combustion-based engines and generators.
- They can be used as a source of power for vehicles thus taking the place of batteries in the transport sector.
- Their size is small and has a compact structure which reduces their weight thus making them suitable for portable applications.

## **Disadvantages and challenges in the way of DMFCs**

### **1.3.1.1 Slow electro-oxidation kinetics**

The electro-oxidation of methanol leads to the formation of many more surface intermediates. Firstly, methanol decomposes to carbon monoxide, COH, HCO, and HCOO. The CO is then oxidized to form CO<sub>2</sub>. Formic acid and formaldehyde are the major byproducts. The process of methanol oxidation slows down when a few of these intermediates do not undergo the process of oxidation but they receive exposure to the surface of the catalyst (poisoning on surface), thereby preventing the surface availability for adsorption of methanol. That step is labeled as a rate limiting step during which the intermediate species are electro oxidized. Sometimes, despite complete oxidation, the efficiency of fuel is reduced that is because some of the intermediates undergo a desorption process followed by their oxidation to CO<sub>2</sub>. Now the main challenge is the development of an electro-catalyst that will be able to prevent adsorption of intermediates causing poisoning of catalyst, increases the reaction rate, and have improved activity for the formation of carbon dioxide.<sup>37</sup>

### **1.3.1.2 Methanol Crossover**

The main purpose of the membrane used between electrodes in PEM fuel cells is to prevent the transfer of oxygen and fuel from one electrode to another electrode where they can undergo a non-electrochemical oxidation reaction. In DMFC, the Nafion membrane allows flow of fuel through it. There exists a concentration gradient between two electrodes so methanol not only by diffusion process but also pulled by the electro-osmotic drag of hydronium ions. Its hydrophilic nature and presence of hydroxyl groups are responsible for its interaction with ion-exchange sites. The Methanol Cross over along with electrons from anode to cathode and oxidized by cathodic oxygen. Consequently, an internal chemical short circuit has been created at the pure platinum cathode that results in current losses. The problem of methanol cross-over could be lessened by reducing the methanol concentration and by elevating the temperature for operation, but these changes are not suitable for micro fuel cells. The technical barrier in the way of DMFCs technology is the Crossover of Methanol (MCO) through membrane towards cathode which has direct effects on the efficiency and working of cell. By changing the thickness and structure of membranes MCO can be controlled. But still, there is a need to develop an active and strong anode catalyst as much of the methanol will be oxidized on the anode preventing its transfer to the cathode. Or cathode catalyst should be modified to a level at which it can tolerate the methanol. Metal (except Pt) based catalysts with zero activity for (MOR) are required.<sup>28,37</sup>

### **1.3.1.3 Management of Heat and other factors**

Another serious problem to be addressed is the control of the heat. There is a direct relation between methanol crossover and temperature. By increasing the concentration of methanol in the anode it eventually increases MCO and temperature. The output voltage of the system is strongly affected by increased reaction kinetics at both electrodes. Only 30% of chemical energy is converted into electrical energy and the remaining energy is dissipated by heat.

In commercializing DMFCs technology many other factors like stability, Durability, cost, and use of many platinum-based catalysts for achieving high energy densities are creating obstacles. The direct methanol fuel cell technology could be made more reliable for both stationary and mobile applications either by reducing the amount of Pt catalyst loaded or by using low cost non-precious metal-based catalysts.<sup>38,39</sup>



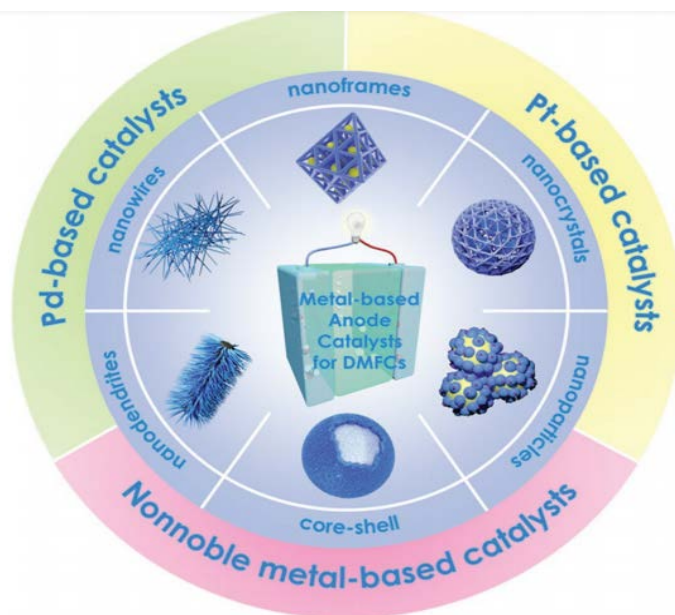
#### 1.4 Electro-oxidation Catalysts for Methanol

Electro-catalysts are listed as a key indicator that has a direct impact on the performance of DMFCs as their reliability is linked to the catalyst used. The main requirement in the DMFCs technology is the development of a catalyst for both electrodes having high efficiency and effectiveness. Several noble metal-based catalysts were developed and at the industrial level, Pt-based catalysts have been utilized as they promoted the catalytic activity, showed higher efficiency, good electrical properties, and stability against corrosion.<sup>40,41</sup> Now researchers are taking much interest to find out other materials having unique features and could be used as a catalyst in place of Pt-metal based catalysts as platinum is a high priced rare metal. The carbon monoxide produced during the methanol oxidation reaction inhibits pure platinum catalysts. Thus, degradation of Pt-catalysts by adsorbed intermediates of CO decreases their lifespan and made them unfavorable for fuel cells. Recent progress in this technology is about developing catalysts having a small amount of platinum. Therefore, various metals such as palladium, ruthenium, Fe, Co, Cu and Ni were alloyed with Pt or platinum was embedded on RuO<sub>2</sub> and MnO<sub>2</sub> metal oxides. The addition of other metals to Pt-catalyst improved their activity for methanol oxidation, developed resistance for CO poisoning thus enhanced the efficiency of the cell.<sup>42</sup>

The stability and charge transfer efficiency of a catalyst were found to be improved by the introduction of conductive support. Two types of support materials have been utilized carbon-based (graphene, activated carbon, and nano-tubes)<sup>43</sup> and non-carbon materials as mesoporous silica and oxides of metals. To make support material suitable for large scale applications it must have some unique characteristics as mentioned below:

- Have good conductivity for electricity
- The surface area should be large
- Strong interaction between catalyst and support
- The structure should be Mesoporous
- Capable of handling water
- Resistant towards CO corrosion

For methanol oxidation reaction the requirement for developing a new catalyst is it should be less expensive, highly active, tolerant to CO poisoning, stable, and easy to prepare.<sup>44</sup>

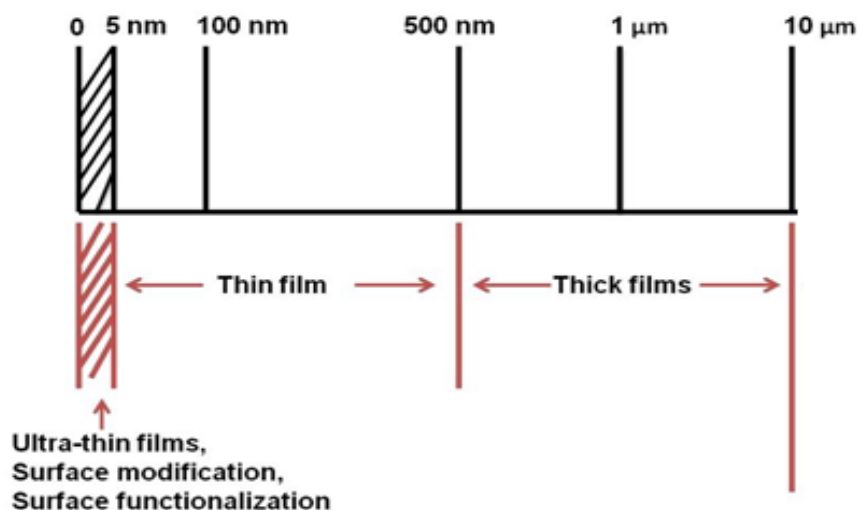


**Figure 8: Reported Electro-catalysts for Oxidation of Methanol**

### 1.5 Metal-oxide thin films

Advances in solid electronics are mainly due to the emerging technology of thin films. The optical properties and activity of semiconductors or ceramics in 2-D structures are responsible for diverting the attention of the world toward thin-film technology. The thickness and geometry of films are studied during the investigation on films formed. Different deposition methods are used for the synthesis of crystalline or amorphous films.<sup>45</sup>

The films having a thickness in the range of 5nm to 2micrometer are called thin films while films having a thickness from 10 to 100micrometers are called thick films. During the deposition process of thin films, the atoms or molecules are deposited individually on the surface. The thick film deposition process involves the deposition of particles. The formation of thin films changes the nature of morphology and structures of the material without causing any change to the bulk material. The specific properties of thin films are due to their metallurgic effect, geometry, microstructure, and increased surface to volume ratio.<sup>46-48</sup>



**Figure 9: Thin Film and Thick Film Rules**

### 1.6 Thin layer deposition techniques

The selection of the method used for the preparation of electro-catalyst is very important as it has a great influence on the activity of the catalyst by shaping their morphology, size, and structure. Other factors that also affect the performance are the solvent used, capping agent, the ability of reactant to be reduced, and the temperature required for preparation. At present, most of the advanced techniques are being utilized for the synthesis of materials having size and thickness in the nanometer range to change their behavior for different applications such as dielectric, electrical, optical, etc. Material science is taking much interest in the development of coatings or thin films. The thin layer of material deposited in the form of thin film has a thickness in the range of nanometers to few micrometers. The nature of the material used and the conditions in which the thin films are synthesized determines their structure may be polycrystalline or amorphous. A substrate on which the layer of material is deposited results in the formation of a thin film. Thin films are maybe single-layered or multi-layered like electrochromic cells or thin-film solar cells. Different deposition techniques used for the fabrication of uniform and unique quality films are listed in **Table 1**<sup>49</sup>

<b>Physical Deposition techniques</b>	<b>Chemical Deposition techniques</b>
<b>1-Evaporation technique</b>	<b>1- Sol-gel technique</b>
a) Vacuum thermal evaporation	<b>2- Chemical bath deposition</b>
b) Electron Beam evaporation	<b>3- Spray pyrolysis techniques</b>
c) Laser beam evaporation	<b>4- Plating</b>
d) Arc evaporation	a) Electroplating techniques
e) Molecular beam epitaxy	b) Electroless deposition
f) Ion plating evaporation	<b>5- Chemical vapor deposition techniques (CVD)</b>
<b>2- Sputtering techniques</b>	a) Low pressure (LPCVD)
a) Direct current sputtering (DC sputtering)	b) Plasma enhanced (PECVD)
b) Radio frequency (RC sputtering)	c) Atomic layer deposition (ALD)

**Table 1 : Different techniques used for deposition**

Some of the fundamental steps which are involved in every deposition technique:

- (i) Synthesis of material to be deposited
- (ii) Material is transported to the substrate
- (iii) Deposition on the surface leads to the growth of film
- (iv) Calcination or annealing according to required properties for films
- (v) Deposition of material on the surface leads to the formation of 2-D surface layers having a thickness in sub-micron that are labeled as thin films.
- (vi) While the formation of coating involves the deposition of particles in the form of layers (thickness > 1microns)

The atoms impinging from the source on the surface of substrate lose energy and get deposited on the substrate through formation of bond with the surface atoms either via van der Waals interactions, metallic bonding or electrostatic interactions (ionic bond). These condensed atoms cluster together to form nuclei. The process of nucleation continues until a thin film of saturated density is obtained<sup>41,46</sup>

### **Dip Coating Method**

Immersion coating is also named as Dip coating deposition technique. Through this method, the material selected for coating is deposited in the form of films on the substrate. Dip coating involves easy steps for the deposition of complex substances as it is a very simple, adaptable, reproducible, and low-cost technique. Dipping can be performed either manually by keeping speed constant or automatically by using dip coater.<sup>51</sup> The dip-coating process involves five major steps for the preparation of films with different thicknesses. 1) At constant speed, the immersion of the substrate in precursor solution which is prepared for coating 2) After some time the substrate is withdrawn from solution keeping the speed same 3) thin film is deposited after the drainage of excess solution from the substrate 4) solvent is evaporated and coated films are dried 5) Sintering /curing of films if required. The concentration of precursor solution is an important factor as agglomeration resulted when higher concentrations of the solution are used. (Figure 10)<sup>52,53</sup>

The process of film formation follows the fluid mechanical equilibrium between the precursor solution and the suspended film. Many forces are playing a very important role in the regulation of mechanical equilibrium such as surface tension, viscous drag, mechanical and electrostatic forces. The thickness and stability during the film formation process are attained by strong adhesive forces and by a balance between draining and entraining forces. Other factors that determine the thickness and properties of deposited films are solution concentration and composition, the viscosity of the solution, angle and time of immersion, speed at which substrate is withdrawn, how many times the process is repeated, temperature, and moisture.<sup>51,54</sup> The equation used for finding out thickness is given below

$$h_0 = c\left(\frac{\eta U_0}{\rho g}\right)^{\frac{1}{2}}$$

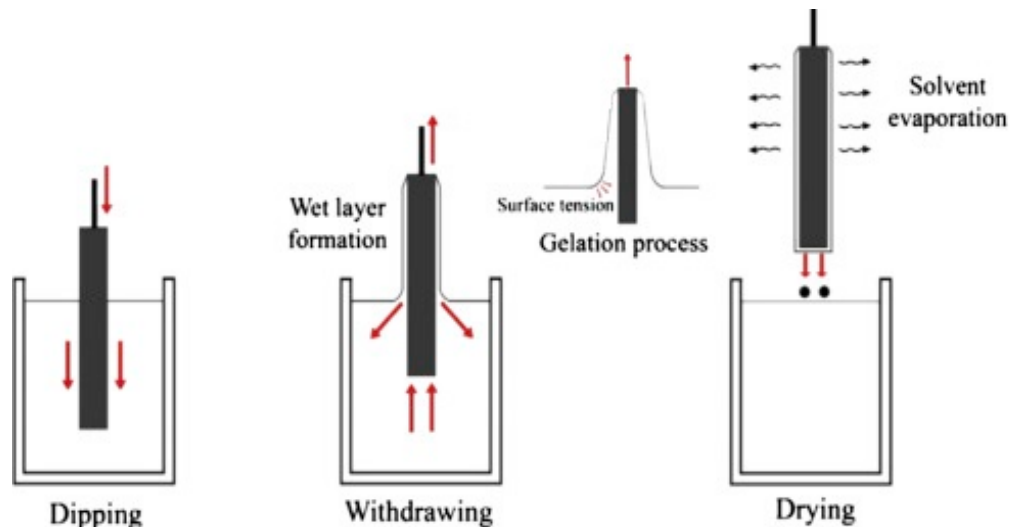
$c$  = constant.

$\eta$  = Viscosity.

$U_0$  = Rate of withdrawal speed of substrate from precursor solution.

$P$  = density of the solution.

$g$  = gravitational constant.



**Figure 10: Schematic representation of steps performed during Dip coating method.**

## AACVD METHOD

Aerosol assisted chemical vapor deposition technique is a modified form of the standard chemical vapor deposition method. The precursor is transported in the form of aerosol droplets/mist to the reaction zone. Gases such as nitrogen, argon, or any other reactive gas are used as carrier for their transport. The AACVD process eliminated the conditions of evaporation and temperature stability of the precursor that will be used for the generation of aerosol from any solvent used. So, it is a very cost-effective process for the synthesis of many CVD products as compared to the chemical vapor deposition process. Advantages of AACVD over CVD method are following:

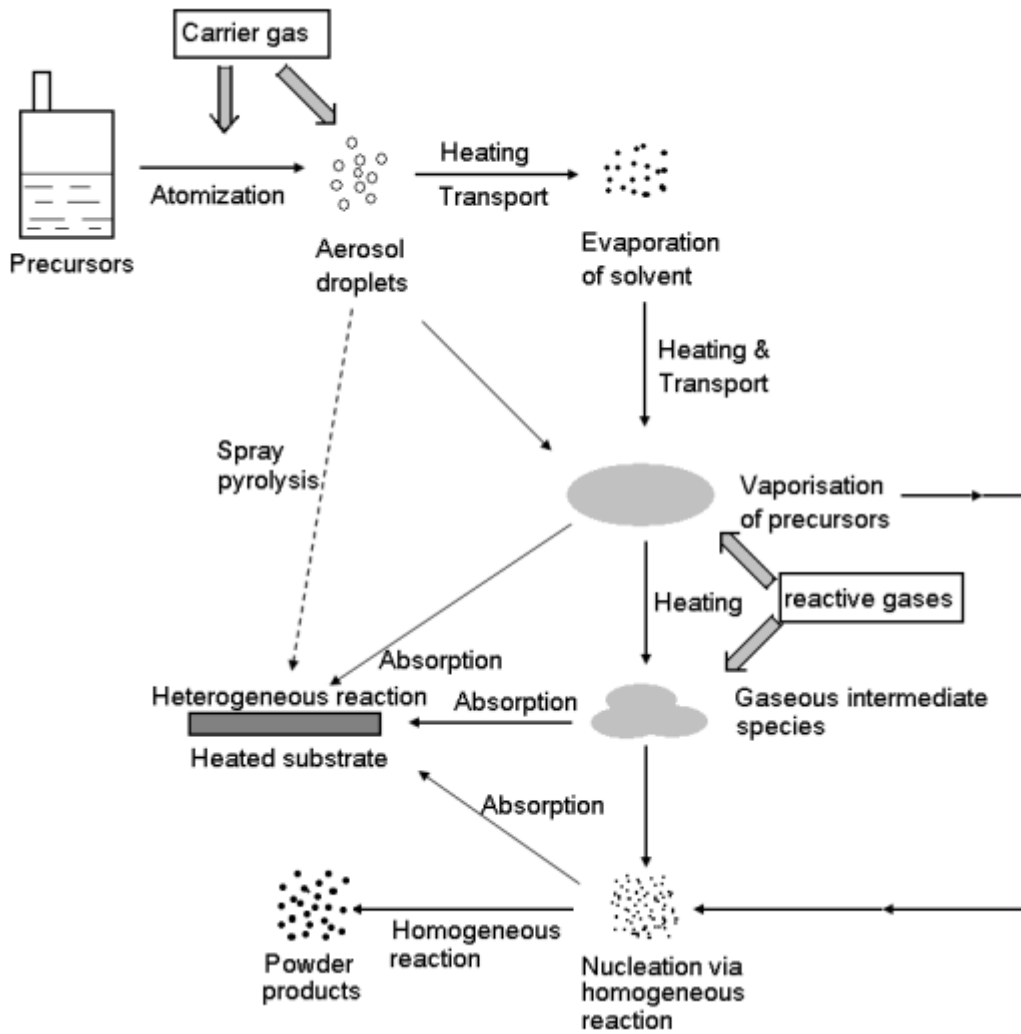
- i) Permits a broad range of precursors that would be used for production of CVD products with improved quality at a low price.



- ii) The formation of aerosol mist from the precursor resolved the problem of its transportation and evaporation.
- iii) The deposition rate is higher due to the higher rate of mass transport of precursor.
- iv) It can be performed in an open environment, and at low or atmospheric pressure.
- v) A simplified method for synthesis of composite materials with controlled stoichiometric composition.<sup>55</sup>

Hence AACVD is a hybrid method having advantages of both techniques spray-pyrolysis and CVD as the precursor is transported as aerosol and deposition follows the mechanism of the CVD deposition process respectively. That's why it is replacing the chemical vapor deposition method in all fields related to the synthesis of products of CVD such as powders, films, nano-tubes, and coatings, etc.

During the AACVD process, the atomization step involves the dissolution of precursor in solvent. Ultrasonic humidifier is used for the generation of aerosol droplets that creates 'precursor mist' that is transported through carrier gas to the heated zone of CVD reactor. Upon reaching the high-temperature zone the solvent starts evaporating /decomposing leaving the precursor in vaporized form. The vaporized precursor undergoes decomposition or other reactions to get deposited on the substrate surface to produce desired substances. ( Figure 11) <sup>56,57</sup>

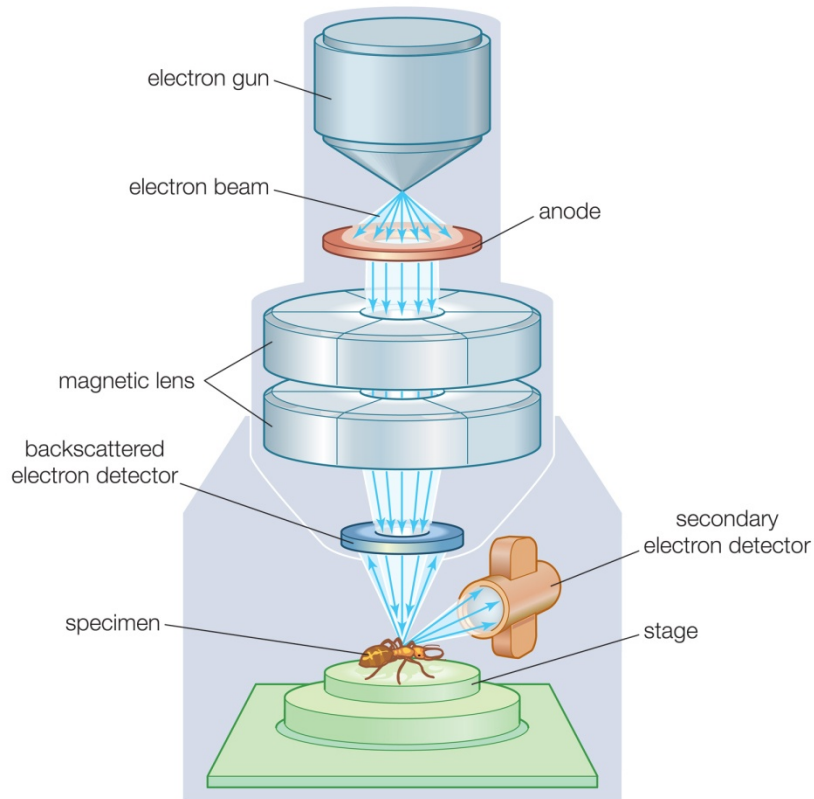


**Figure 11: Schematic diagram of AACVD method**

## 1.7 Characterization techniques

### Scanning electron microscope (SEM)

Scanning electron microscope (SEM) is an instrumental technique commonly used for imaging and analysis of surface morphology and microstructures of solid materials. For the investigation of particle size, this method is preferred because it has a resolution power of 100 Å. With the advancement in technology recently used SEM instrument has attained the resolution of 25 Å which can be used along with energy-dispersive X-ray microanalysis techniques for compositional and crystallographic analysis. The electrons and photons are emitted from the surface of the sample as a result of different interactions which occurs when a beam of low-energy electrons passes through the sample.<sup>58,59</sup> The interaction between electrons and material results in the production of signals that are received and detected by the detector to generate an image of a sample. For the characterization of materials, several modes of SEM are available for example, secondary electrons imaging, electron channeling, Auger electron microscopy, X-ray mapping, and backscattered electrons imaging. In which mode the SEM is in use determines the type of detector required for that mode. The figure is showing the different parts of a typical scanning electron microscope<sup>60</sup>



© 2012 Encyclopædia Britannica, Inc.

**Figure 12: Different parts of Scanning Electron Microscope**

### **X-Ray Diffraction Spectroscopy (XRD)**

X-ray diffraction (XRD) is used for finding out the nature (crystalline or amorphous) of materials. In 1912, Max von Laue revealed that in the wavelength range for X-rays the crystalline materials behave as 3D diffraction grating just like the atomic spacing of crystalline planes in a lattice. Now this simple and non-destructive technique is in common use for the investigation of unknown crystal structures and spacing of atoms in a lattice. XRD pattern is obtained by constructive interference as a result of interaction between X-rays and crystalline samples. The Cu  $K\alpha$  radiation ( $\lambda = 1.5406 \text{ \AA}$ ) is used as a source of X-rays. From a cathode ray tube, the X-rays are generated, converted to monochromatic rays by passing through monochromators, then they are concentrated towards the sample by using collimator. With the satisfaction of Bragg's law, constructive interference occurs, and a diffraction peak is produced.

Bragg's law:

$$2d\sin\theta = n\lambda$$

$\lambda$ = wavelength

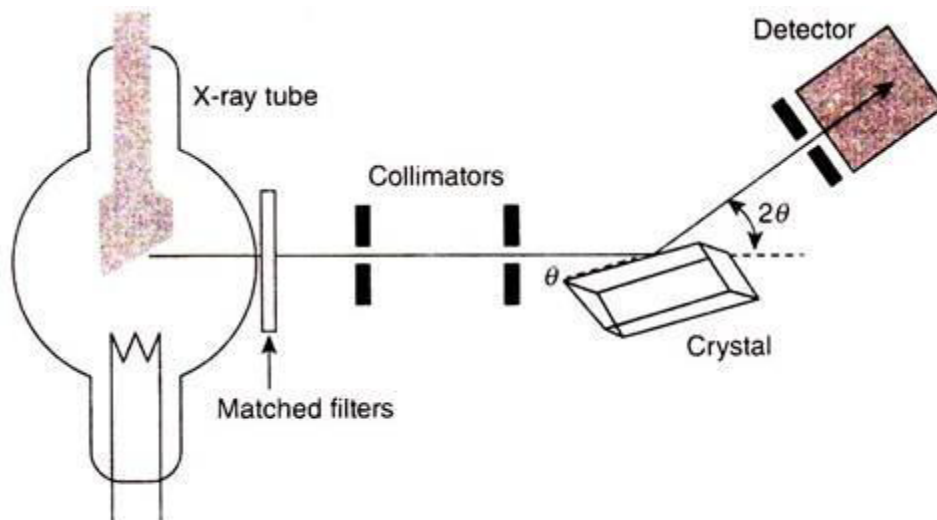
d= interlayer distance

n= no. of layers under consideration

Main components are:

- i. X-ray tube
- ii. Sample holder
- iii. X-ray detector
- iv. X-ray diffractometer.

Radiations are diffracted at different angles according to the orientation of planes in a lattice that's why the sample is scanned in a specific 2-theta range. After collection at detector the diffracted signals undergo further processing which involves their conversion to count rate which is then displayed on the computer as output. How the atoms are arranged in a crystal lattice of sample is reflected by its distinctive XRD pattern which serves as a fingerprint of that sample. The position of atoms in lattice planes of material is used for the determination of peak intensity. The sample under investigation must be homogenous, well-grounded with average size composition. This method provides details about the crystalline phases, structure, texture, other parameters of lattice for example average size of the grain, defect in a crystal, crystallinity, Epitaxy, strain. In the case of thin films, it is used to measure their thickness.<sup>61</sup>



**Figure 13: Illustrative Diagram of X-Ray Diffractometer**

### **Fourier Transform Infrared Spectroscopy (FT-IR)**

Fourier Transform Infrared Spectroscopy is also named FT-IR spectroscopy. An advanced molecular spectroscopic technique that has found its applications in the characterization of polymers, carbon containing compounds, and some non-organic materials. It is not sensitive to the physical state of the sample. During FT-IR analysis radiation from the infrared region is used for scanning samples and their chemical properties. Infrared radiations in the range of 10,000 to 100  $\text{cm}^{-1}$  from the source when passes through sample some of them got absorbed and other are emitted. The molecules of the sample generate vibrational or rotational energy from adsorbed radiations. The final signal collected by the detector is represented in the form of an Infrared- spectrum (4000  $\text{cm}^{-1}$  to 400 $\text{cm}^{-1}$ ). As each molecule has a specific functional group that's why IR-spectrum is considered as a fingerprint of that molecule this makes the identification of samples easier. This material analysis technique is used for smaller particles (10 -50 microns) for determining their composition.

- FTIR analysis is used for the identification and characterization of:

- Unknown materials (e.g., solids, liquids, powders, or films)
- Contaminations present in the material
- Identification of additives obtained as extraction product of a polymer matrix
- Identification of oxidized, decomposed, or untreated monomers <sup>62</sup>

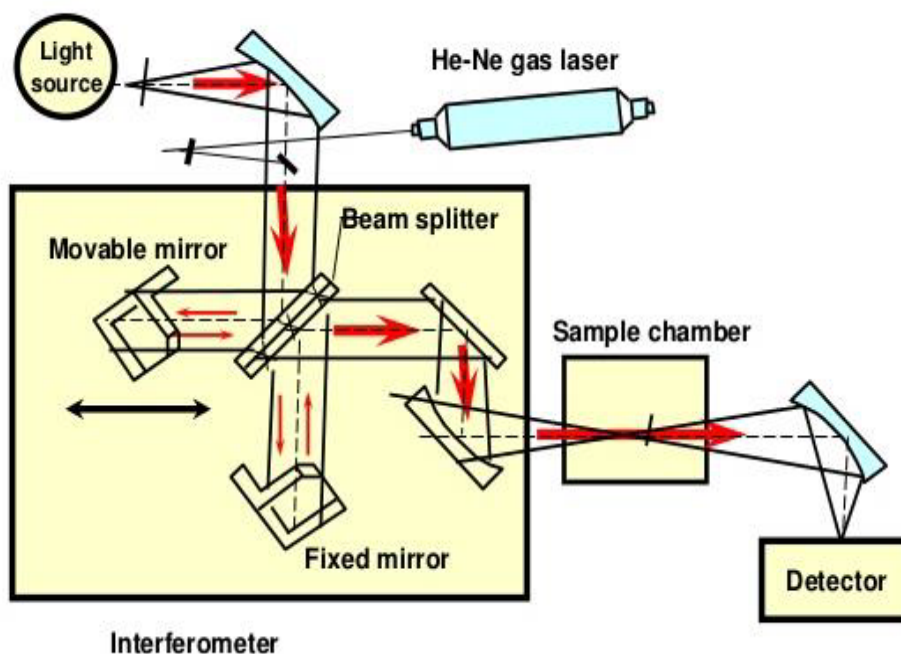
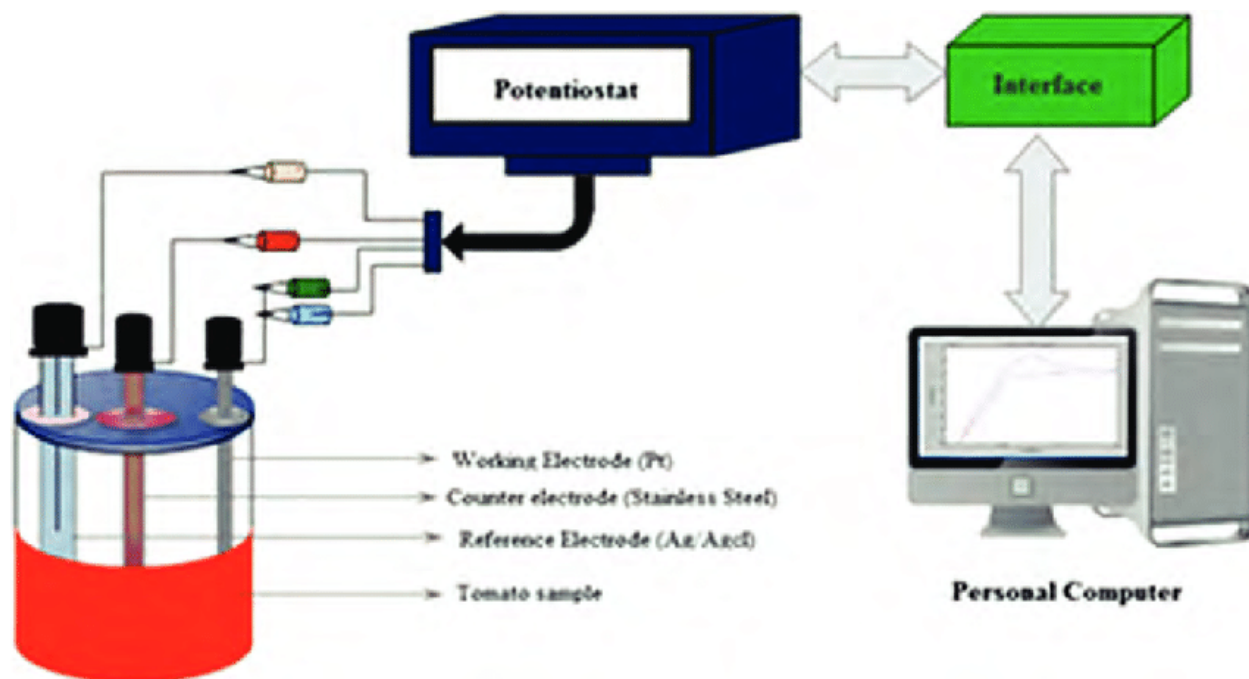


Figure 14: Illustrative diagram of FT-IR

## 1.8 Electrochemical techniques:

### Cyclic voltammetry (CV)

An electrochemical method labelled as Cyclic voltammetry (CV) involves the investigation of the mechanism during which redox reactions occurs at electrodes, diffusion coefficients, and standard rate constant of electron transport. This technique is suitable for testing the electro-activity of species. It has become the most common electro-analytical technique in biochemistry, inorganic, organic, and electrochemistry because it is simple and highly adaptable.



**Figure 15: Schematic-representation-of-measurement-setup-of-cyclic-voltammetry**

The CV setup is used for analyzing the electrochemical properties of the analyte in the form of a solution.

The electrochemical cell system with three electrodes:

1. Working electrode
2. Counter electrode – Pt wire
3. Reference electrode- Ag/AgCl

Potentiostat is used for monitoring the potential applied between electrodes i.e. working and reference. The process continues until it approaches that limit at which it is swept back. The device in real-time is used for measuring the changing current between the counter probe and working electrode as this process is repeated many times throughout a scan. A cyclic voltammogram is obtained in the form of a duck-shaped plot. The cyclic voltammogram is a plot of potential versus current. During the potential scan, the current is measured at the working electrode to obtain the Cyclic voltammogram.



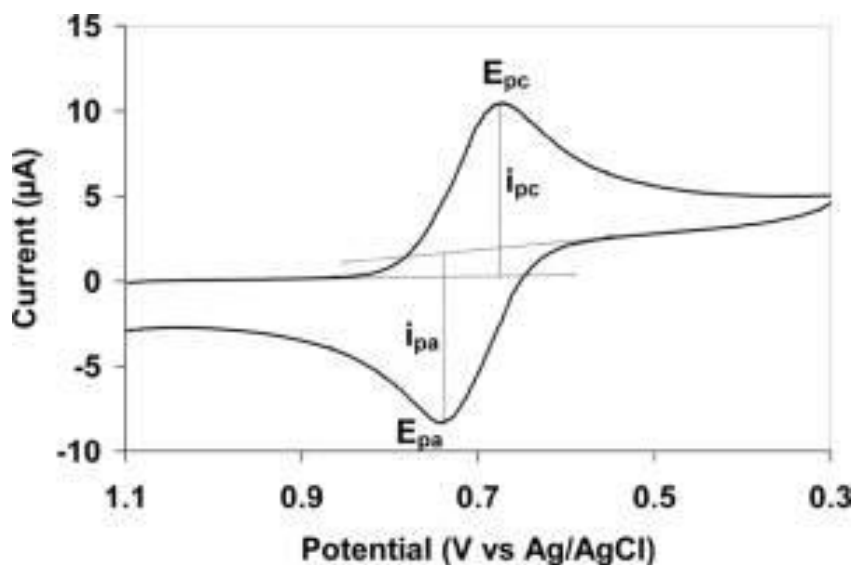


Figure 16: Conventional Cyclic Voltammogram

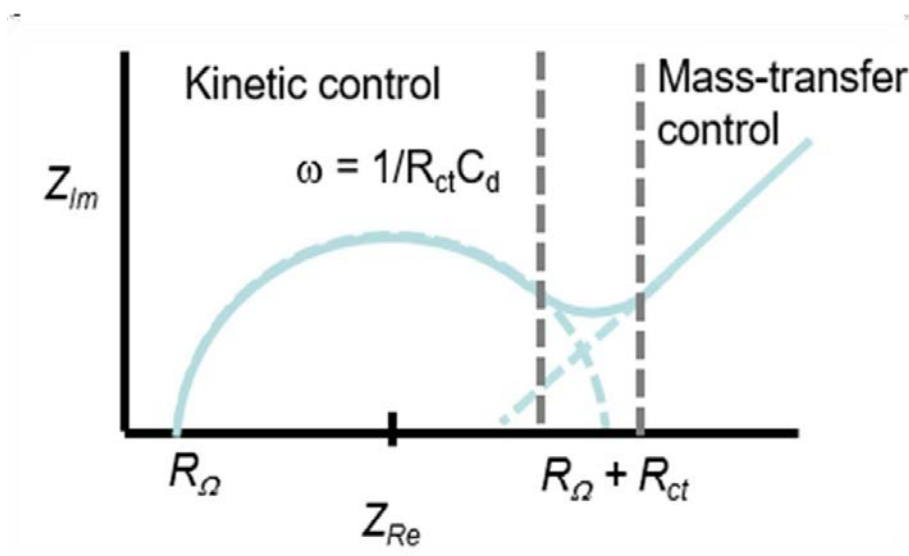
The type of working electrode used is very important as it enhances the surface adsorption of materials and gives a specific potential window. The working electrodes are selected according to the experiment performed. The electrode with constant potential and equilibrium is taken as reference electrode and the potential of other electrodes is measured in comparison to it. The reference electrodes which are in common use are Saturated Calomel Electrode (SCE), Standard Hydrogen Electrode (SHE), and Ag/AgCl electrode. The electrical circuit is completed when a wire (Pt) or disk is used as counter electrode. Solution's conductivity is directly related to the electrolyte concentration. Although electrons are generated at electrodes and they are transferred through an electrolyte to keep the charge-balanced.<sup>63,64</sup>

### Electrochemical Impedance Spectroscopy (EIS)

To what extent a circuit can resist the flow of current is measured in terms of impedance. Impedance is a resistance that depends on frequency. An AC potential is applied to the cell and current is measured to calculate the impedance.

$$Z\omega = E\omega/\omega$$

For EIS measurements, at a fixed frequency range the sinusoidal voltage or current is applied, and response is recorded at each frequency. The EIS data presentation is either in the form of a Bode plot or Nyquist plot. The Nyquist plot is preferred over the Bode plot for impedance measurements. Two modes are available i.e., potentiostatic and galvanostatic mode for running EIS setup that is similar to cyclic voltametric setup.



**Figure 17: Electrochemical Impedance Spectroscopy (Nyquist Plot)**

The information obtained from impedance analysis can be used for; differentiation of electrochemical processes, identification of diffusion-controlled processes, capacitive behavior of the electrodes, rate of electrochemical reaction, and for corrosion study of metallic electrodes.<sup>65</sup>

## 1.9 Objectives



### *Research Objective*

Synthesis of ceramic thin films by Aerosol Assisted Chemical Vapor Deposition (AACVD) & Dip coating method.

Optimization of different parameters such as concentration, Scan rate and Temperature

Characterization of synthesized electro-catalyst via XRD, Raman Spectroscopy, SEM-EDS and AFM.

Study of electrochemical activity of synthesized catalyst through cyclic voltammetry for Methanol oxidation.

Measurement of charge transfer parameters.

## 2 CHAPTER 02

### LITERATURE REVIEW

**Danaee et al. [2008]** synthesized Ni oxide films on electrodeposited Ni and Ni-Cu alloy on glassy carbon surface by an electrochemical deposition method. In order to investigate oxidation-reduction reactions and their electrocatalytic role in alkaline solutions, CA and CV techniques were used. The cyclic-voltametric analysis of Ni-Cu alloy indicated the appearance of Ni oxyhydroxide  $\beta/\beta$  crystallographic form under repetitive cycling in alkaline media. When 0.3molar CH<sub>3</sub>OH was added the Ni-Cu/GC catalyst showed higher value of current density in comparison to Ni/GC at 650mV vs Ag/AgCl. This improvement in methanol oxidation in the presence of modified Ni-Cu alloy electrode has been attributed to larger surface area of Ni oxyhydroxide. With the increase in current for anodic peak decrease in current for cathodic peak was observed. The anodic peak current of Ni-Cu/GC was found to be in direct relation to square root of scan rate. The results of CA analysis were confirming the CV measurements as the diffusion coefficient value for methanol oxidation obtained was  $2 \times 10^{-6} \text{cm}^2 \text{s}^{-1}$ .<sup>66</sup>

**R.M. Abdel Hameed et.al [2010]** examined the electro-oxidation of methanol using carbon electrodes having coating of Nickle-Phosphorus and Nickle-Copper-Phosphorus and in KOH solution. Electroactivity was measured by performing CV and CA. The influence of parameters selected for deposition was also examined on catalytic activity as these catalysts were prepared by electroless deposition methods. The variations in time required for deposition, temperature and pH were observed. A smooth structure with solid surface was exhibited by SEM analysis. After addition of Cu the amount of Ni and phosphorus was decreased which was confirmed by EDS analysis. Copper/Nickel oxyhydroxide species were used to escalate the effectiveness of Nickel-Copper-Phosphorous/Carbon catalyst. Furthermore, they shut down the g-NiOOH phase and stabilized the b-NiOOH phase. Catalyst which was prepared by electroless deposition method at temperature of 90°C and pH 9.0 showed highest electrocatalytic activity.<sup>67</sup>

**Qiu, J. D. et al. [2011]** presented a very convenient and manageable way for production of Platinum particles highly dispersed on graphene functionalized with poly- (diallyldimethylammonium chloride) (PDDA) via single step  $\text{NaBH}_4$  reduction process. The mass ratio of PDDA-GO to  $\text{H}_2\text{PtCl}_6$  was kept under control to achieve uniform distribution of nanoparticles on surface within required range 18-78wt-percent. For the characterization of Pt/graphene nano-composites different techniques including energy dispersive spectrometry (EDS), transmission electron microscopy (TEM), X-ray diffraction (XRD) spectroscopy, and thermogravimetry analysis (TGA) were used. These prepared Pt nanocomposites are dispersed in graphene, showing significant electro catalytic activity and resilience in dealing with CO toxicity in methanol oxidation. This proposed method was proved as good for the development of catalysts that are most effective in making the fuel cells valuable.<sup>68</sup>

**Muhammad Adil Mansoor et al. [2013]** used heterobimetallic molecular complex,  $[\text{PbTi}(\mu\text{-O}_2\text{CCF}_3)_4(\text{THF})_3(\mu\text{-O})]_2$  (1) as single source precursor for the synthesis of Perovskite-structured  $\text{PbTiO}_3$  thin films. Glass substrate coated with FTO were selected as substrate and method used was Aerosol-assisted chemical vapor deposition. Precursor complex was synthesized under optimum conditions by simple reaction of tetraacetatolead(IV), tetrabutoxytitanium(IV), and trifluoroacetic acid in THF and then characterization was done by microanalysis, FT-IR, XRD, and thermal analysis. The precursor complex was found to be unique as all the components required for lead titanate were present in single structure and decomposes at  $550^\circ\text{C}$  when subjected to AACVD process. Well-grained thin films of  $\text{PbTiO}_3$  were deposited with glassy appearance and thickness of 340 nm. For the characterization of films different techniques were used. From UV-visible spectrophotometry analysis the 3.69 eV value was obtained for optical band gap. These thin films with lowest size are preferred for photo-electrical and photo-catalytic applications<sup>69</sup>

**Yingying Gu et al. [2015]** used thermal decomposition process for the synthesis of Ni-Cr electro-catalyst. TEM and XRD characterization of these electro-catalysts shows that at extreme temperature of  $< 700^\circ\text{C}$ , the mixture of NiO and  $\text{Cr}_2\text{O}_3$  have rhombohedral structure and the Ni-Cr nano-particles with average size of 30-40nm have uniform dispersion. In order to investigate their electro-activity for methanol oxidation in alkaline solution containing 1.0 M MeOH CV and CA analysis was performed. As compared to NiO nano-catalyst the Ni-Cr nano-catalyst showed improved electro-catalytic activity and appeared more stable in NaOH solution for methanol

oxidation. The current density value was  $12.6\text{mAcm}^{-2}$  for Ni-Cr nano-oxide electrode. It is the synergistic effect between Ni and Cr oxides that is responsible for enhanced electro-catalytic activity of prepared Ni-Cr nano catalyst. Due to high current density value, stability in NaOH solution and better tolerance towards CO, for methanol oxidation, Ni-Cr oxide nano-catalyst are more efficient and these are relatively more cheaper as compared to others.<sup>70</sup>

**H. B. Hassan et al. [2016]** prepared Ni - MgO nanocomposites to carbon anodes where there are positive particles of MgO stabilization by electrodeposition from a nickel Watts bath. In comparison to pure Ni coated on carbon (Ni/C) their electro catalytic efficiency was tested for oxidation of alcohol in an alkaline solution. The deposited nanocomposites were identified by XRD, SEM along with EDS analysis. Their electro catalytic activity was estimated by performing different electrochemical studies including CA, CV and EIS. Improvement in the activity of pure Nickel catalyst designed for electro-oxidation of alcohol was due to insertion of MgO. High current density values are obtained with Nickel-MgO/Carbon electrode. The Ni-MgO/C electrode which was prepared at optimum current density  $40\text{mAcm}^{-2}$  exhibited anodic peak current  $176\text{mAcm}^{-2}$  for ethanol and  $196\text{mAcm}^{-2}$  for methanol. The cyclic Volta-metric measurements were confirmed by EIS results revealing decrease in resistance to charge transfer and roughness of Ni-MgO/C electrode was increased.<sup>71</sup>

**Sohail Ahmed et al. [2014]** reported the synthesis of an octa-nuclear heterobimetallic complex  $[\text{Y}_2\text{Cu}_6\text{C}_{10.7}(\text{dmac})_6(\text{OAc})_{7.3}(\text{OH})_4(\text{H}_2\text{O})_2] \cdot 3\text{H}_2\text{O} \cdot 0.3\text{CH}_3\text{C}_6\text{H}_5$  1(dmac=dimethylaminoethanoate; OAc =acetato). Different techniques were used for the characterization of complex formed including, XRD, FT-IR, and melting point. Then complex was subjected to deposition to form thin films of  $\text{Y}_2\text{CuO}_4\text{-CuO}$  at extreme temperature using AACVD method. SEM, XRD and EDX studies to investigate the morphology and composition of thin films indicate that octa-nuclear heterobimetallic composite have even distribution of particles. These particles were in range of 19-24nm size with band gap energy of 1.82 eV and photocurrent density of  $9.8\mu\text{Acm}^{-2}$  at 0.80Vvs SCE. The thin films synthesized can not only be used for photochemical but also for solar cell applications as they appeared to be as photoactive and can generate electrons and holes.<sup>72</sup>

**Muhammad Adil Mansoor et al. [2014]** used AACVD method for the deposition of  $\text{Mn}_2\text{O}_3\text{-4TiO}_2$  composite thin films on FTO coated glass substrate in a solution of freshly prepared hex nuclear single source molecular precursor  $[\text{Mn}_2\text{Ti}_4(\text{TFA})_8(\text{THF})_6(\text{OH})_4(\text{O})_2] \cdot 0.4\text{THF}$  1 (where TFA = trifluoroacetato and THF = tetrahydrofuran). Elemental analysis, FT-IR, ( $^1\text{H}$  NMR) spectroscopy, (TG/DTG) and single crystal X-ray analysis were performed for the characterization of precursor molecule. Morphological features and composition of synthesized films was examined by XRD, SEM along with EDX. The results showed that the composite of  $\text{Mn}_2\text{O}_3\text{-4TiO}_2$  has uniform distribution of particles size that range between 112-308nm. They also noted the optical band gap energies of 1.20 and 2.8qeV with photocurrent density of 3431Ua/cm<sup>2</sup>. The synthesized material was accepted as good for solar energy and photochemical applications.<sup>73</sup>

**Jing-Jia Zhang et al. [2017]** used simple sintering process for the synthesis of  $\text{MoO}_3\text{-C}$  composite co-support for the Pt-based anode catalyst. In electrocatalytic field the  $\text{MoO}_3\text{-C}$  composite is used as support for catalysts regardless of its non-conduction property it is highly active and stable. The Pt/ $\text{MoO}_3\text{-C}$  catalyst was fabricated by depositing Pt nanoparticles on the  $\text{MoO}_3\text{-C}$  substrate for their possible use in electro-oxidation of methanol. Nanoparticles are successfully incorporated into the  $\text{MoO}_3\text{-C}$  substrate to form a Pt /  $\text{MoO}_3\text{-C}$  catalyst for electro-oxidation of methanol. The results of electrochemical analysis highlighted that using the catalyst Pt/ $\text{MoO}_3\text{-C}$  increase the stability plus activity in methanol oxidation compared to others. This increase in catalytic performance was due to strong link between the metal and Pt installation support as there were more active sites on  $\text{MoO}_3\text{-C}$  support and dispersion of Pt nanoparticles was also uniform. The  $\text{MoO}_3\text{-C}$  support acts as electronic promoter for PT-catalyst thus the Pt/ $\text{MoO}_3\text{-C}$  catalyst could be used for fuel cell applications.<sup>74</sup>

**M. A. Mansoor et al. [2017]** first time the synthesized of thin films of trimetallic [Fe, Mn, Ti] oxide composite photocatalyst with  $\text{Fe}(\text{OAc})_2$  and bimetallic manganese-titanium complex. They used aerosol-assisted chemical vapor deposition technique. They characterized the thin film with different X-ray and spectroscopy techniques. Functioning of catalyst was investigated via photo electrochemical oxidation of water. Furthermore, PEC analysis of film at low voltage of 0.20V, shows the photocurrent density of 1.88mAc<sup>2</sup>.

The results were further confirmed by EIS analysis. The Mott-Schottky plot indicated the flat band potential of - 1.0 V vs Ag/AgCl.<sup>75</sup>

**M. A. Mansoor et al. [2017]** synthesized thin films of ceramic composite CdO-Mn<sub>2</sub>O<sub>3</sub>. They applied the AACVD method for deposition of films on fluorine doped Tin oxide coated glass substrate and used 1:1 mixture of cadmium complex and diacetatomanganese. For structure, thickness and other activities, they used XRD, FT-IR, spectroscopy studies. FEG-SEM results indicate the effects of solvent on the morphology of synthesized films. When THF was used as solvent the optical band gap obtained was 1.95 eV. Photocurrent density was dependent on deposition medium and n-type behavior was exhibited by CdO– Mn<sub>2</sub>O<sub>3</sub> composite semiconductor electrode. Maximum photocurrent density of 4.80 mA cm<sup>-2</sup> at 0.65 V vs. Ag/AgCl/3M KCl (~1.23V vs. RHE) in 0.5 M NaOH electrolyte was observed for films fabricated from THF solution.<sup>76</sup>

**Su Pei Lim et al. [2014]** designed silver deposited Titania (Ag/TiO<sub>2</sub>) nanocomposite film by using AACVD method. They noted photocurrent density of 1mAcm<sup>2</sup> at modified electrode of Ag/TiO<sub>2</sub> under simulated solar AM1 5G irradiations (100mW/cm<sup>2</sup>). The deposition of silver, increase the charge transfer process on surface of TiO<sub>2</sub> that resulted in enhancing the photo electrocatalytic performance. Density functional theory (DFT) calculations indicate the adsorption of methanol at Ag surface of electrode via electron transfer. The adsorption of methanol on Ag surface of Ag/TiO<sub>2</sub> through transfer of electrons from silver to methanol. On TiO<sub>2</sub> surface optimal concentration of Ag was measured as 5 mM.<sup>77</sup>

**H.B. Hassan et al. [2018]** used metal oxides to enhance the electrocatalytic performance of Ni for the electrooxidation of alcohols. They used electrodeposition method for the synthesis of Ni metal oxides (Fe<sub>2</sub>O<sub>3</sub>, ZnO, Co<sub>3</sub>O<sub>4</sub> and MnO<sub>2</sub>) nanocomposites on carbon electrode. As an electrode these catalysts were used in the electrooxidation of ethanol and methanol and their efficiencies were calculated. The composition and morphology of prepared nanocomposites were determined by EDX, XRD and SEM analysis. Chronoamperometry, cyclic voltammetry and impedance spectroscopy were used to investigate the electrocatalytic activities of these nanocomposites. As compared to Ni/C these modified nanocomposites were more stable with improved catalytic



activity and low resistance to charge transfer. According to their performance for electrooxidation they were arranged in following order Ni-Fe<sub>2</sub>O<sub>3</sub>/C > Ni-ZnO/C > Ni-Co<sub>3</sub>O<sub>4</sub>/C > Ni-MnO<sub>2</sub>/C > Ni/C. The prepared nanocomposites have mixed oxides and synergistic effect among them was responsible for the increasing the catalytic performance of catalysts. The Ni- Fe<sub>2</sub>O<sub>3</sub>/C catalyst showed maximum value of current densities 302 and 339mAcm<sup>-2</sup> for 1.0M ethanol and 1.0M methanol respectively. For ethanol and methanol electrooxidation the Ni- Fe<sub>2</sub>O<sub>3</sub>/C catalyst exhibited low values of R<sub>ct</sub> as 10.7 and 6.2Ω cm<sup>2</sup> and after 50 cycles its efficiency was 93% for methanol and 89% for ethanol. These Ni-metal oxide nanocomposites are best to use as electro catalyst for direct alcohol fuel cell applications.<sup>78</sup>

**Zohreh Merati et al. [2017]** reported the synthesis, characterization and application of Pt-nanoparticles on metal oxide support materials (SnO<sub>2</sub>, Sb and Nb doped SnO<sub>2</sub>). Simple electrodeposition method was used for their preparation and characterized by field-emission scanning electron microscopy (FESEM) and energy dispersive X-ray analysis (EDX). The CV analyses were performed to test their electrocatalytic activity when they were used as an electrode for oxidation of methanol and CO which were absorbed on Pt. The CV and CA measurements indicated that in acidic media the Pt/Sb-SnO<sub>2</sub>/Ti and Pt/Nb-SnO<sub>2</sub>/Ti electrodes were more stable and exhibited enhanced catalytic activity than Pt/Ti and Pt/SnO<sub>2</sub>/Ti electrodes. The SnO<sub>2</sub> acts as a sink of electron that resulted in increasing the conduction of electrons. Thus, catalyst performed more proficiently when SnO<sub>2</sub> was doped with Nb and Sb, result in increased surface area for electrochemical and methanol oxidation surface area and methanol oxidation activity. These SnO<sub>2</sub> doped catalysts acceptable as electrocatalyst for electrooxidation of methanol and have direct application in methanol fuel cells industry.<sup>79</sup>

**Jacob E. Robinson et al. [2018]** reported oxide-encapsulated metal electrocatalyst SiO<sub>x</sub>|Pt based on the membrane-coated electrocatalyst (MCEC) architecture for oxidation of alcohols in acidic media. During the process of CO stripping voltammetry, the SiO<sub>x</sub> MCECs showed less onset potentials of CO oxidation and maximum current density was increased twice as compared to Pt. The proximal hydroxyls of silanol groups interact with adsorbed intermediates on Pt and these interactions are responsible for the improvement in the electrocatalytic activity for methanol

oxidation in acidic electrolyte. Thus, advantage of using MCEC design on interfacial region is that plenty of hydroxyl groups are available at SiO<sub>x</sub>|Pt interfaces and promotes the oxidation of alcohol by following bifunctional mechanism. The silanol groups were the major participants in the oxidation of methanol and confirmed by CV and pH measurements.<sup>80</sup>

**Khadija Munawar et al. [2018]** introduced a single- source precursor [Y<sub>2</sub>Ti<sub>2</sub>(u<sub>3</sub>-O)<sub>4</sub>(u<sub>2</sub>-O(H<sub>2</sub>O)(TFA)<sub>8</sub>(THF)<sub>5</sub>]. Using the AACVD method, it can be used for the fabrication of Y<sub>2</sub>Ti<sub>2</sub>O<sub>7</sub>-2TiO<sub>2</sub> base thin films on fluorine-doped tin oxide substrates at extreme temperature. Fabricated films were characterized by SEM, EDX, XRD and XPS analysis. The results confirmed the formation of pure and high quality crystalline Y<sub>2</sub>Ti<sub>2</sub>O<sub>7</sub>-2TiO<sub>2</sub> composite films like mesoporous micro balls. According to PEC experiments, when OH<sup>-</sup> ion concentration was increased the photocurrent density. There was increase in photocurrent to its maximum value of 60 μAcm<sup>-2</sup> with band gap energy of 1.8eV at pH of 13.5. Furthermore, PEC analysis about CA indicated that Y<sub>2</sub>Ti<sub>2</sub>O<sub>7</sub>-2TiO<sub>2</sub> thin films have more stability against photocorrosion.<sup>81</sup>

**Muhammad Adil Mansoor et al. [2019]** used [Mn<sub>2</sub>Zn<sub>2</sub>(TFA)<sub>8</sub>(THF)<sub>4</sub>]<sub>n</sub> (1) complex for the fabrication of MnZnO<sub>3</sub> thin films through assisted chemical vapor deposition. Using the field emission gun- scanning electron microscope, an agglomerated flower-like structure was shown in films for oxidation and stoichiometric calculations of each element was determined by X-ray photoelectron microscopy. For oxidation of methanol the photocatalytic activity of as prepared MnZnO<sub>3</sub> films was tested. Maximum of photocurrent density of 2mAcm<sup>-2</sup> was observed in the presence of 0.6M methanol solution at MnZnO<sub>3</sub> photoelectrode. It is three times than the value obtained when methanol was not added.

The CA analysis indicated that deposited films have greater resistivity and stability against photo corrosion in alkaline media. EIS measurements revealed that when small amount of methanol was added it got oxidized and reduced the charge transfer resistance value to 395.5 Ω.<sup>82</sup>

**Kemal Volkan Özdokur et al. [2018]** for the first time reported the TiO<sub>2</sub>/ZnO/Pt nanocomposite film as electrocatalytic surface to improve methanol oxidation in alkaline medium. DC sputtering followed by electro-deposition method was used for the preparation of TiO<sub>2</sub>/ZnO on FTO substrate. After that on prepared nanocomposite films the Pt nanoparticles were fabricated. To

investigate the structure and function of film different characterization techniques and electrochemical analyses were performed.  $\text{TiO}_2/\text{ZnO}$  composite films were found to have wurtzite ZnO layers and anatase  $\text{TiO}_2$  with a thickness of 320 and 370nm. Best catalytic activity was observed when ZnO and Pt nanoparticles deposition process completed its 5 cycles. For  $\text{TiO}_2/\text{ZnO}/\text{Pt}$  electrode at a voltage of  $-0.17$  V the oxidation peak of 0.5 M methanol was observed and the corresponding peak current was increased about 10- and 5-fold in comparison to FTO/Pt and FTO/ $\text{TiO}_2$ /Pt electrodes, respectively.<sup>83</sup>

## 3 CHAPTER 03

### EXPERIMENTAL WORK

#### 3.1 Materials

The chemicals which were used for the synthesis of NiO-Mn<sub>2</sub>O<sub>3</sub>@FTO and NiO-(MgO-ZnO) @FTO composite thin films were of analytical grade. Further purification was not required before using them. Inorganic salts such as Nickel (II) acetate dihydrate [Ni (CH<sub>3</sub>COO)<sub>2</sub>.2H<sub>2</sub>O], Manganese (II) acetate tetrahydrate [Mn(CH<sub>3</sub>COO)<sub>2</sub>.4H<sub>2</sub>O], Zn(II) acetate dihydrate [Zn(CH<sub>3</sub>COO)<sub>2</sub>.2H<sub>2</sub>O], and Magnesium(II) acetate tetrahydrate [Mg(CH<sub>3</sub>COO)<sub>2</sub>.4H<sub>2</sub>O], were purchased from sigma Aldrich. Sodium hydroxide [NaOH], Methanol (99.8% pure), Ethanol (99.8%), Trifluoroacetic acid [TFA], acetone and commercially available fluorine Tin oxide coated glass [FTO] were also the products of sigma Aldrich. Doubly distilled water was used for washing and preparation of solutions.

#### 3.2 Instruments

Hot plate, Digital weight balance, Sample drying oven, Ultrasonication bath, Magnetic stirrer, Chamber furnace, Heating oven, Tube furnace, Humidifier, and electrochemical potentiostat.

#### 3.3 Apparatus

Pipette, measuring cylinders, Beakers, glass spatula, glass vials, syringe (3ml, 5ml, 10ml), China dish, Forceps, FTO glass substrate (1\*2cm pieces), two neck round bottom flask.

#### 3.4 Methodology

##### Preparation of precursor's solution

##### 3.4.1.1 Preparation of solution for NiO-Mn<sub>2</sub>O<sub>3</sub>

After taking known amounts of these salts( Ni(OAc)<sub>2</sub>.2H<sub>2</sub>O & Mn(OAc)<sub>2</sub>. 4H<sub>2</sub>O), they were dissolved in solvent (methanol) in order to prepare their 0.1M solutions separately. At room temperature the solutions were stirred for 15 minutes until they got cleared. Also 0.1M solution for mixture (NiO-Mn<sub>2</sub>O<sub>3</sub> 1:1) of these salts was prepared by taking their known amounts and

stirring was performed for 15 minutes. For comparative analysis, same procedure was followed for preparation of solutions having different concentration ratio of these salts.

#### **3.4.1.2 Preparation of solution for NiO-(Mg-ZnO)**

A solution (0.5g by weight) of three salts  $\text{Ni}(\text{OAc})_2 \cdot 2\text{H}_2\text{O}$ ,  $\text{Zn}(\text{CH}_3\text{COO})_2 \cdot 2\text{H}_2\text{O}$ , and  $\text{Mg}(\text{CH}_3\text{COO})_2 \cdot 4\text{H}_2\text{O}$  (1:1:1) was prepared by adding their known amounts in 15ml of methanol. Few drops of Trifluoroacetic acid (TFA) were added to solution to completely dissolve the salts. Then solution was left for magnetic stirring for 15-20 minutes at room temperature.

#### **Synthesis of metal oxide composite (NiO-Mn<sub>2</sub>O<sub>3</sub>/FTO) thin films**

Dip coating method was used for the deposition of NiO-Mn<sub>2</sub>O<sub>3</sub> thin films on glass substrate FTO. A mixture of acetone, ethanol and iso-propanol was prepared for cleaning purpose of FTO. The mixture containing fluorine tin oxide films [ $2 \times 1 \text{ cm}^2$  ( $1 \times w$ )] was placed in Ultrasonication water bath for sonication at room temperature for 40 minutes. As the washing process for FTO films was completed they were dried and kept in ethanol solution. Firstly, the bare FTO films were dipped in as prepared 0.1 M precursor solution of Ni-Mn mixture for 30 seconds then they were placed on hot plate for drying at 120°C for 10 minutes. As a result of this process first layer was deposited and the same film was dipped again in same precursor solution for 30 seconds and then they were placed on hot plate for drying at 120°C for 10 minutes, second layer was deposited. For the ultrafine and uniform deposition of films on the FTO same process was repeated five times. The deposited films were placed in chamber/ muffle furnace for calcination at 500°C for 3hours. For comparison purpose separate films of nickel oxide and manganese oxide were also fabricated by performing the same procedure.

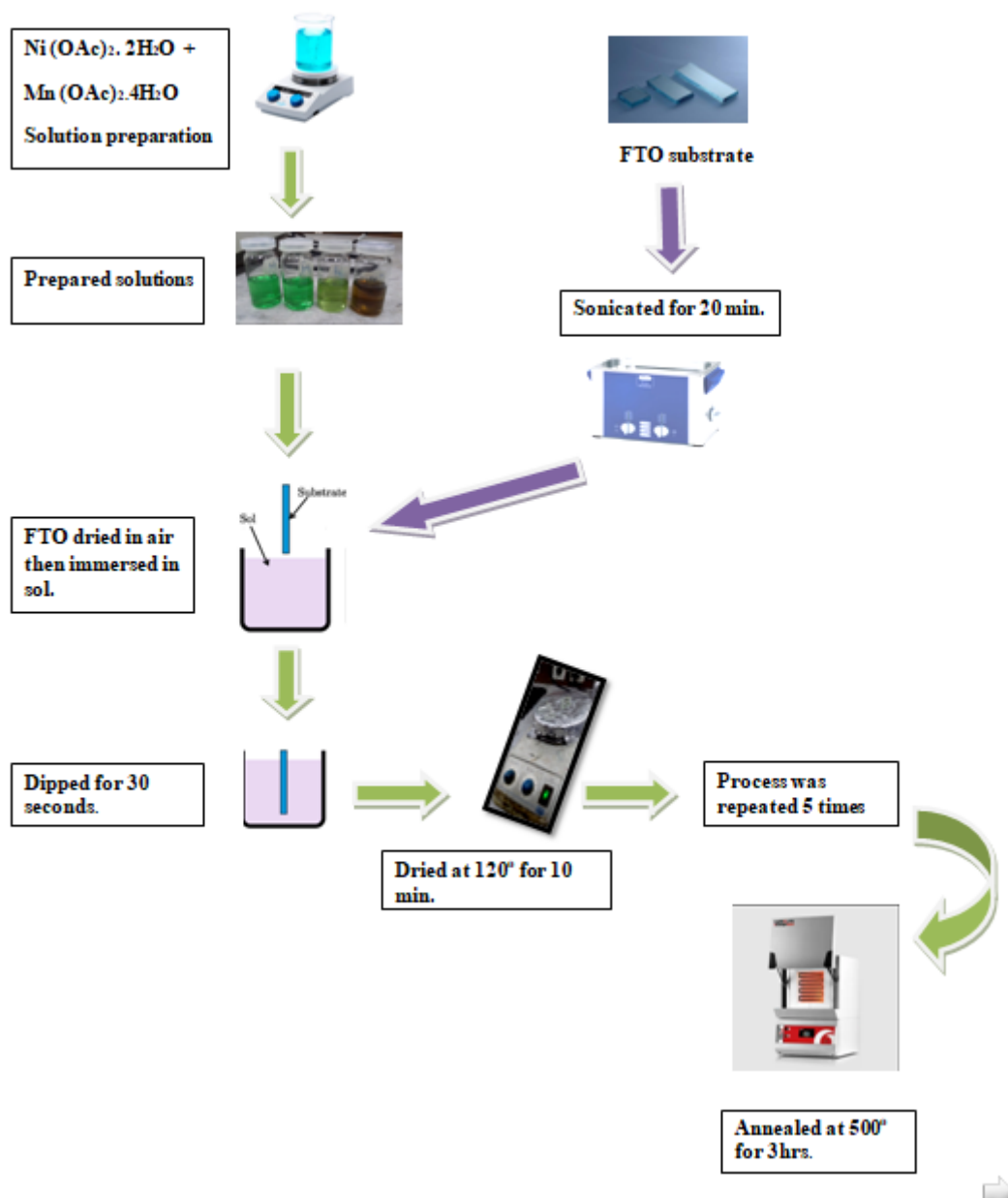


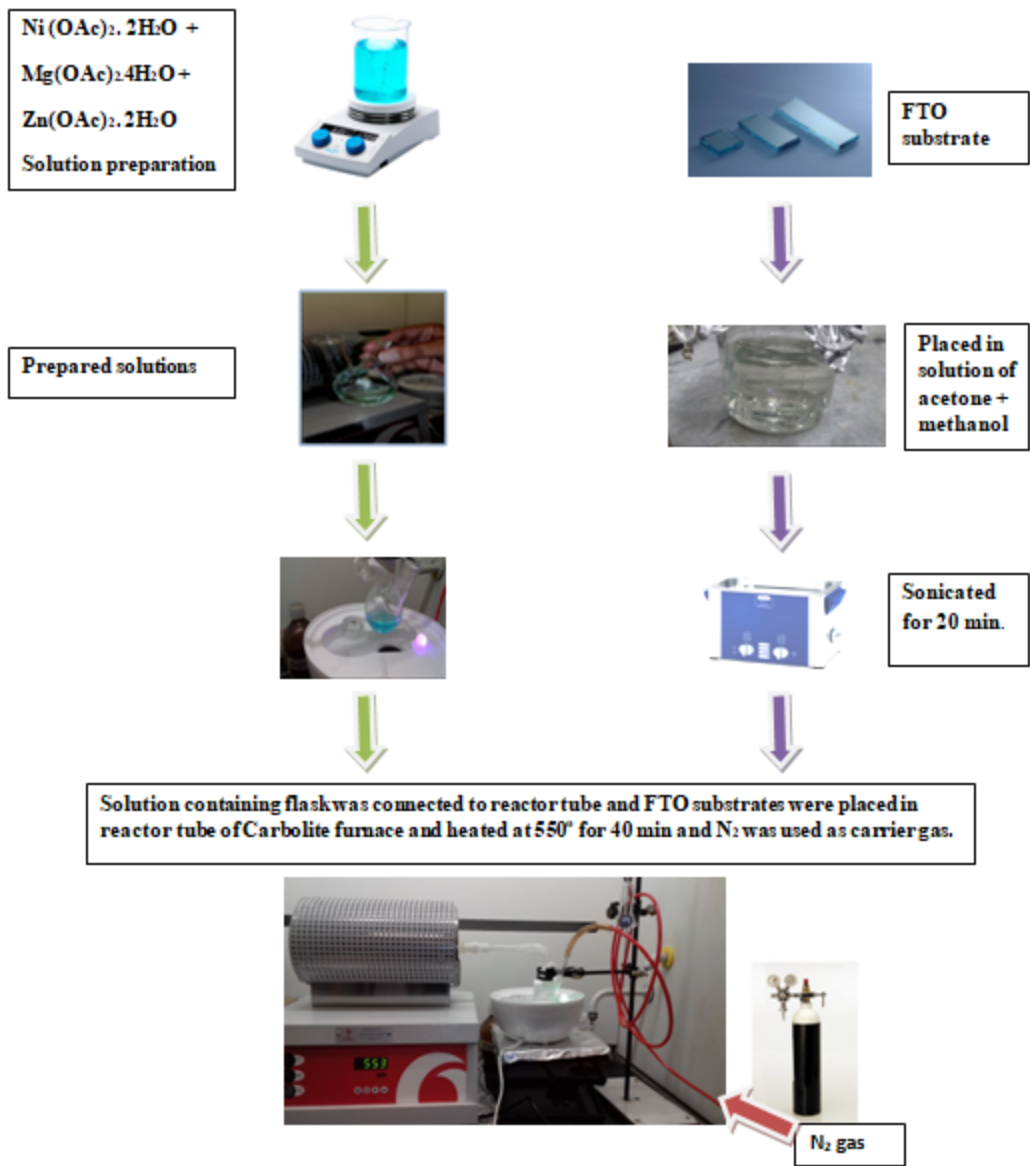
Figure 18: Schematic representation of metal oxide composite thin films synthesis via dip coating method.

Sr. No.	Thin Films	Precursor	Molarity(M)	Solvent
1.	NiO/FTO	Ni(OAc) <sub>2</sub> .2H <sub>2</sub> O	0.1	Methanol
2.	Mn <sub>2</sub> O <sub>3</sub> /FTO	Mn(OAc) <sub>2</sub> .4H <sub>2</sub> O	0.1	Methanol
3.	NiO- Mn <sub>2</sub> O <sub>3</sub> /FTO	Ni(OAc) <sub>2</sub> .2H <sub>2</sub> O & Mn(OAc) <sub>2</sub> .4H <sub>2</sub> O	0.1 0.1	Methanol Methanol

**Table 2: Synthesized metal oxide thin films**

### **Synthesis of metal oxide composite (NiO-(Mg-ZnO)/FTO) thin films**

AACVD method was used for the fabrication of NiO-(MgO-ZnO) composite thin films on FTO(glass substrate). The FTO substrate [2×1cm<sup>2</sup> (1×w)] were washed and dried at room temperature. Then they were placed in reactor tube of Carbolite furnace. The prepared solution was moved to two necked-round bottom flask (100mL) with gas inlet and other side of flask was linked to reactor tube. Carrier gas was used for the transport of aerosols generated from solution. The flow rate for N<sub>2</sub> carrier gas was maintained at 120-130mL. Flask containing the prepared solution was placed in water bath above piezoelectric ultrasonic humidifier. Precursor aerosol droplets are produced and transported by carrier fuel to the hot spot of the reactor tube. As they came in contact with heated surface of FTO substrate they were thermally deposited in the form of films at 550°C. This thermal deposition process took 40 minutes to complete. The NiO-(Mg-ZnO)/FTO composite thin films were also deposited at 400°C and 500°C.



**Figure 19: Schematic representation of synthesis of NiO-(Mg-ZnO) films on FTO by AACVD method.**

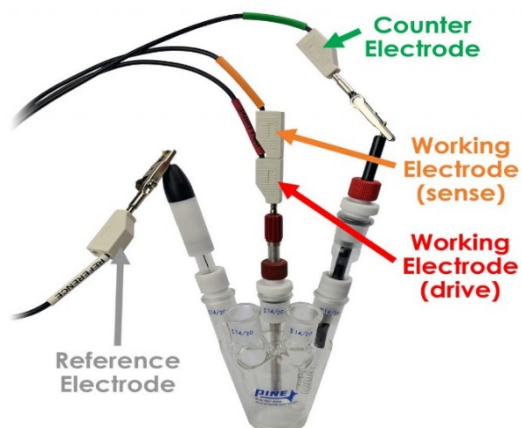


Sr. No.	Thin Films On FTO substrate	Precursor	Molarity(M)	Solvent	Temperature
1.	NiO-(Mg-ZnO)	Ni(OAc) <sub>2</sub> .2H <sub>2</sub> O, Mg(OAc) <sub>2</sub> .4H <sub>2</sub> O, Zn(OAc) <sub>2</sub> .2H <sub>2</sub> O	0.1	Methanol + Few drops of Trifluoroacetic acid	550 °C
2.	NiO -(Mg-ZnO)	Ni(OAc) <sub>2</sub> .2H <sub>2</sub> O, Mg(OAc) <sub>2</sub> .4H <sub>2</sub> O, Zn(OAc) <sub>2</sub> .2H <sub>2</sub> O	0.1	Methanol + Few drops of Trifluoroacetic acid	500°C
3.	NiO-(Mg-ZnO)	Ni(OAc) <sub>2</sub> .2H <sub>2</sub> O, Mg(OAc) <sub>2</sub> .4H <sub>2</sub> O, Zn(OAc) <sub>2</sub> .2H <sub>2</sub> O	0.1	Methanol + Few drops of Trifluoroacetic acid	400°C

**Table 3 : Metal oxide composite (NiO-(Mg-ZnO)/FTO) thin films at different temperatures**

### **3.5 Applications of prepared composite thin films in the electrochemical oxidation of Methanol**

Electrochemical potentiostat (Gamry G750) was used to study the electrocatalytic activity of films subjected to methanol oxidation. The potentiostat consisted of three electrodes embedded in an electrolyte solution. The Pt wire acted as a counter electrode, incorporating metal oxide films as the active electrode and Ag / AgCl as the reference electrode.



**Figure 20: Electrochemical Cell consisting of three electrodes**

In 0.5M NaOH electrolyte solution the electro catalytic activity was studied at scan rate of 100 mV/s in the absence and presence of methanol. The methanol was added to the electrolyte solution with the difference of 0.2 up to maximum concentration 1.4 molar methanol. The effectiveness of fabricated composite oxide films was determined by performing linear sweep voltammetry (LSV), Cyclic voltammetry (CV), chronoamperometry (CA) and electrochemical impedance spectroscopy (EIS) measurements. Moreover, by keeping experimental conditions same the catalytic performance of the deposited thin films for electro-oxidation of methanol was also investigated at different scan rates in order to make comparison.



**Figure 21: Potentiostat for Electrochemical Studies**

## 4 CHAPTER 04

### RESULTS AND DISCUSSION

#### 4.1 Characterization of (NiO-(Mg-ZnO)//FTO) and NiO- Mn<sub>2</sub>O<sub>3</sub> /FTO) thin films

##### Energy Dispersive X-Ray Spectroscopy (EDX)

Energy-dispersive X-ray spectroscopy is a chemical microanalysis technique which uses X-rays for mapping the elements. It gives information about elemental composition and how they are distributed throughout the material. The EDS spectra of films NiO-(Mg-ZnO)/FTO synthesized by AACVD method are represented in Figure 22 and the spectra of films NiO, Mn<sub>2</sub>O<sub>3</sub>, and NiO-Mn<sub>2</sub>O<sub>3</sub> which are synthesized by Dip coating method are shown in Figure 23. The required elements appeared in the respected spectra, and their appearance confirms the formation of films.

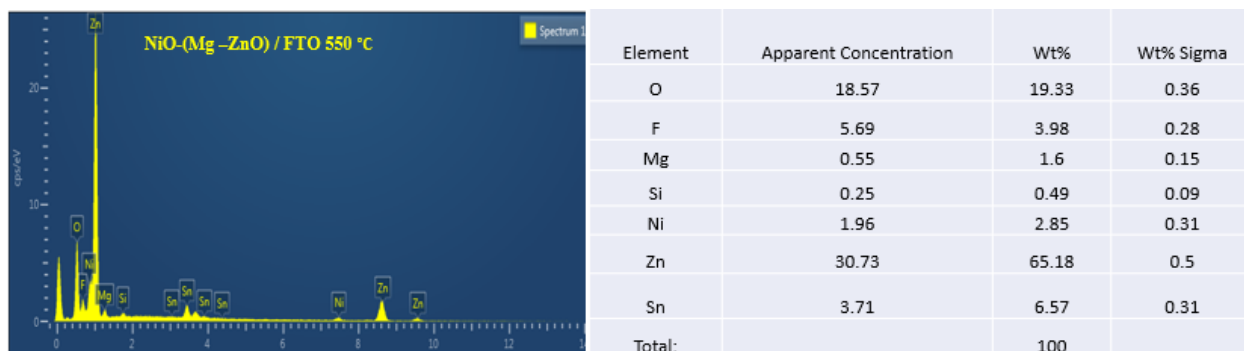
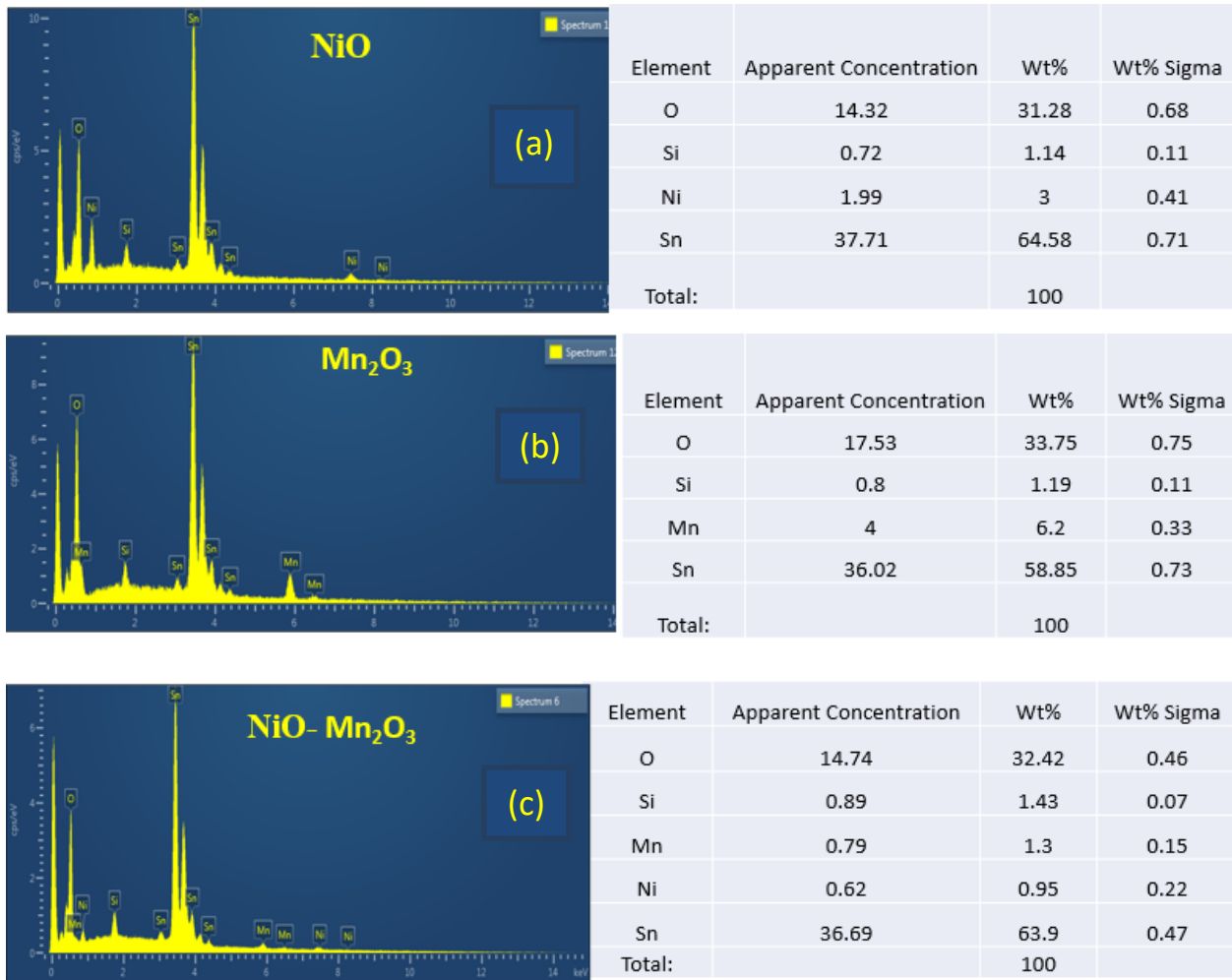


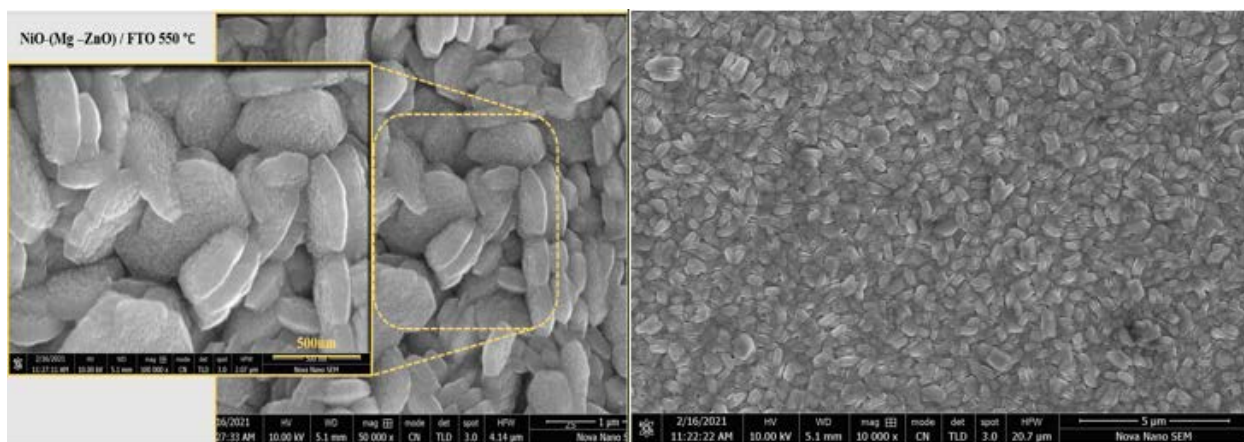
Figure 22: EDS spectra of NiO-(Mg-ZnO)/FTO thin films with Table 4 in which atomic and weight percent of elements are mentioned.



**Figure 23: EDS spectra of a) NiO b) Mn<sub>2</sub>O<sub>3</sub> c) NiO- Mn<sub>2</sub>O<sub>3</sub>**

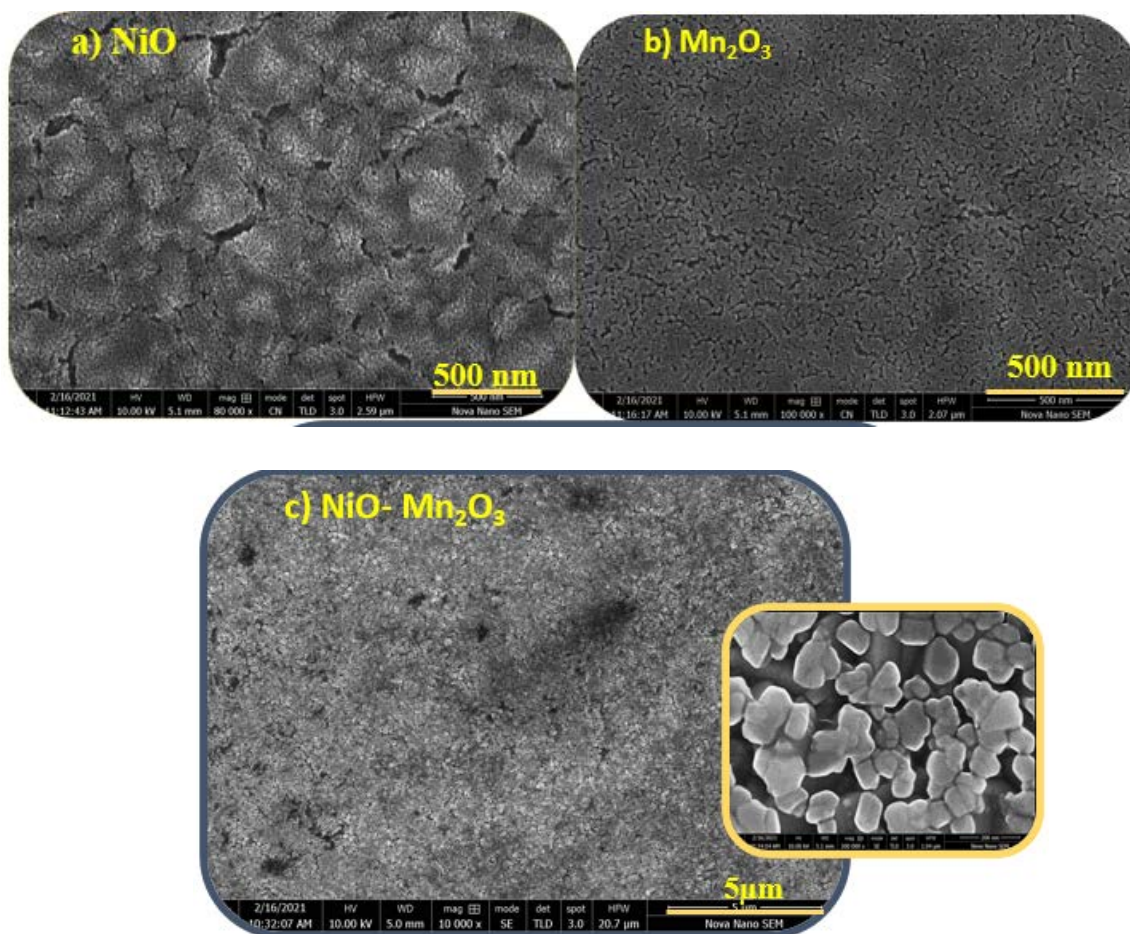
### Scanning Electron Microscopy (SEM) Analysis

Scanning Electron Microscopy (SEM) is a powerful investigation tool. An electron beam is used for scanning the sample's surface. It is designed for production of highly magnified (2-D) images of sample and characterization of surface morphology. Figure 24 represents the SEM images of thin films NiO-(Mg-ZnO)/FTO 550 °C. It is clear from images that surface of thin films is dense and particles are interconnected to form an agglomerate. The size and shape of agglomerates are irregular. The average size of agglomerate is 440nm.



**Figure 24: SEM images NiO-(Mg-ZnO)/FTO films.**

The SEM images of NiO/FTO, Mn<sub>2</sub>O<sub>3</sub>/FTO, NiO-Mn<sub>2</sub>O<sub>3</sub>/FTO are shown in Figure 25. It is evident from image of NiO-Mn<sub>2</sub>O<sub>3</sub>/FTO thin films that particles are uniformly distributed throughout the surface. The surface is smooth and porous which helps in the movement of electrolyte solution and methanol to reach deep down layers of catalyst and hence improves the efficiency and kinetics of methanol oxidation reaction. The average particle size of NiO-Mn<sub>2</sub>O<sub>3</sub>/FTO thin films is 95nm.

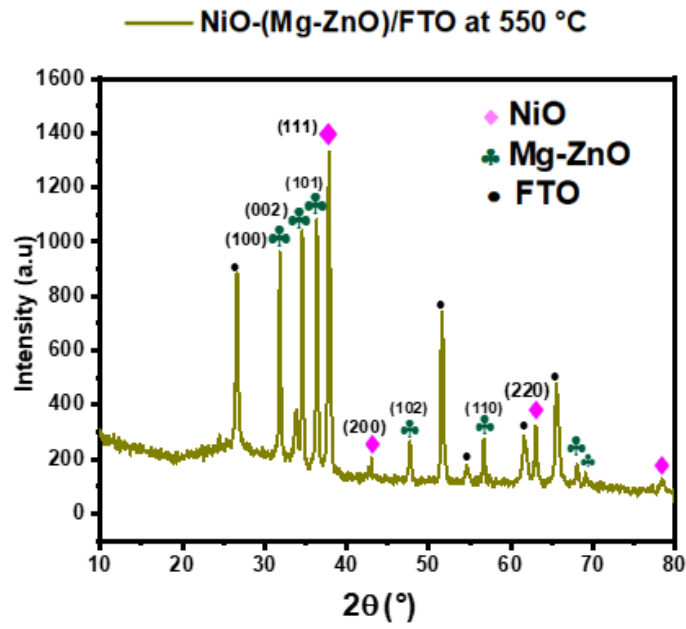


**Figure 25: SEM images of a) NiO b) Mn<sub>2</sub>O<sub>3</sub> c) NiO- Mn<sub>2</sub>O<sub>3</sub>/FTO thin films.**

### **X-Ray Diffraction (XRD) analysis**

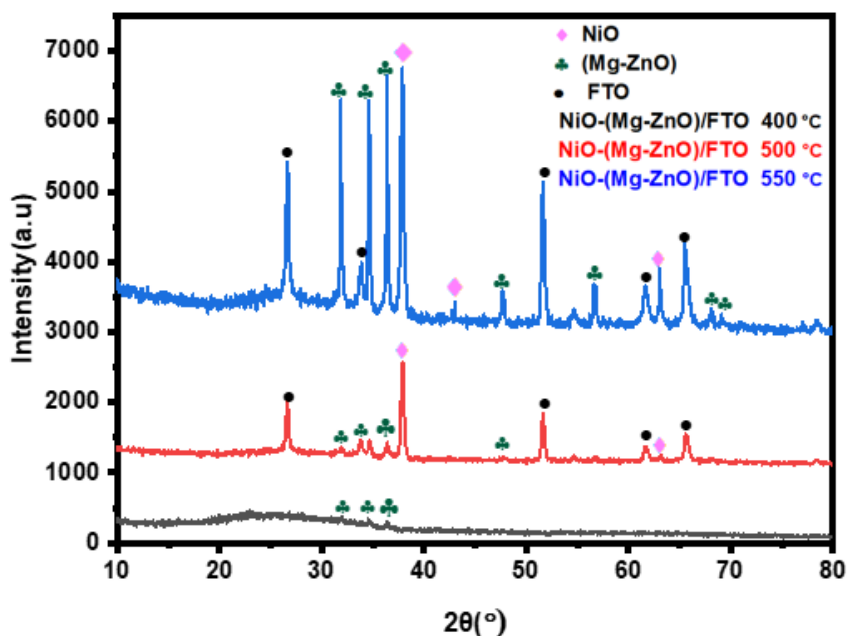
XRD technique is used for investigation of crystallographic features of synthesized films. The XRD spectra for NiO-(Mg-ZnO)/FTO 550°C is represented in the Figure 26. After subtraction of peaks for FTO substrate (JCPDS 00-001-0657) the remaining peaks appeared individually and confirming the presence of cubic NiO ( $2\theta = 37.8^\circ, 43.3^\circ, 63^\circ$  with corresponding planes (111), (200), (220) and Wurtzite Hexagonal structure for Mg doped ZnO ( $2\theta = 33.8^\circ, 34.6^\circ, 36.3^\circ, 47^\circ, 56^\circ, 68^\circ$  having plane orientations (100), (002), (101), (102), (110) and (201). They are best match with reference cards (JCPDS # 00-004-0835) for NiO and (JCPDS card no. 00-036-1451) for Mg-ZnO. The average crystallite size is 43nm which is calculated by using Debye Scherrer equation. The comparison XRD spectra for thin films NiO-(Mg-ZnO)/FTO produced at various temperatures

(400°C, 500°C ,550°C) is given in Figure 27. It is evident from spectra that peaks become prominent, and crystallinity improves with increase in temperature.



**Figure 26: X-ray Diffraction pattern of NiO-(Mg-ZnO)/FTO thin films.**

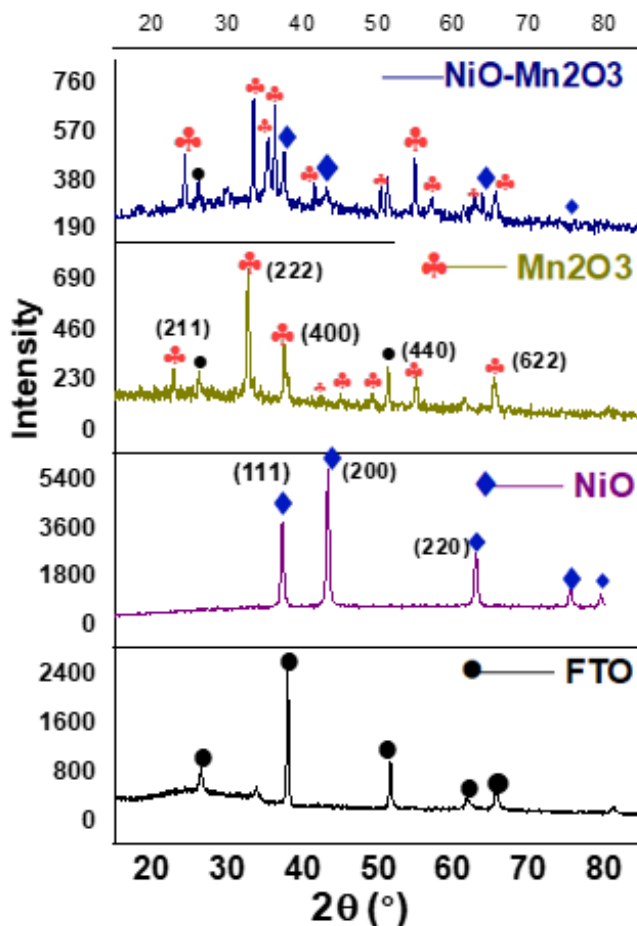




**Figure 27: Comparison of X-ray Diffraction pattern of NiO-(Mg-ZnO)/FTO thin films synthesized at various Temperatures a) 400°C b)500°C c)550°C.**

The XRD spectra for NiO, Mn<sub>2</sub>O<sub>3</sub>, NiO-Mn<sub>2</sub>O<sub>3</sub>/FTO thin films are represented in Figure 28. The diffraction peaks at  $2\theta = 37.2^\circ, 43.3^\circ, 62.9^\circ, 75.5^\circ, 79.4^\circ$  are referring to cubic structure of NiO. These peaks are perfect match with reference card 01-073-1523 for crystalline cubic NiO. The prominent peaks for Mn<sub>2</sub>O<sub>3</sub>/FTO thin films appeared in XRD spectra with plane orientations (211), (222), (400) and (440) and exact match with reference spectra of cubic Mn<sub>2</sub>O<sub>3</sub> (card # 01-078-0390). The X-ray diffraction pattern for NiO-Mn<sub>2</sub>O<sub>3</sub>/FTO thin films exhibiting that, peaks appeared separately for face centered cubic NiO and Cubic crystal plane structure for Mn<sub>2</sub>O<sub>3</sub> with peak positions ( $2\theta = 24.3^\circ, 26.2^\circ, 30^\circ, 33^\circ, 35^\circ, 36^\circ, 37.4^\circ, 41^\circ, 43^\circ, 50^\circ, 51^\circ, 54^\circ, 57^\circ, 62^\circ, 63^\circ, 65^\circ, 76^\circ$ )<sup>84,85</sup>. The average crystallite size is calculated from Debye-Scherrer equation which is 32nm, 33nm and 36nm for NiO/FTO, Mn<sub>2</sub>O<sub>3</sub>/FTO and NiO-Mn<sub>2</sub>O<sub>3</sub>/FTO thin films respectively.



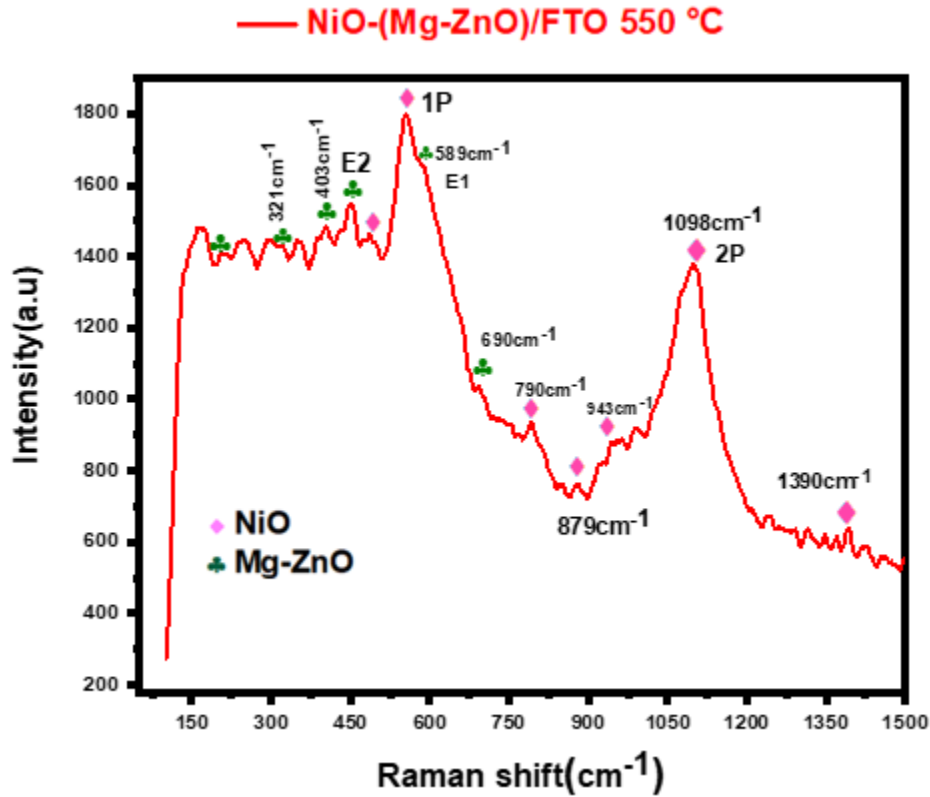


**Figure 28: X-ray Diffraction pattern of NiO/FTO, Mn<sub>2</sub>O<sub>3</sub>/FTO, NiO-Mn<sub>2</sub>O<sub>3</sub>/FTO thin films.**

### **Raman Spectroscopic analysis**

Raman spectroscopic analysis was also performed to confirm the formation of ceramic thin films. In Figure 29 Raman spectra of NiO-(Mg-ZnO)/FTO thin films has been shown. Two main vibrational bands at  $556\text{cm}^{-1}$  and  $1098\text{cm}^{-1}$  appeared confirming the cubic phase structure of NiO. These bands are due to first (1P) and second (2P) order phonon scattering and corresponds to longitudinal (LO) and 2LO components respectively. A sharp peak at  $450\text{cm}^{-1}$  is non-polar Raman active  $E_2$  (High) mode which confirms the hexagonal structure of Mg-ZnO. The long range electrostatic order is confirmed by peak at  $588\text{cm}^{-1}$  which is labelled as  $E_1$  (LO) optical mode that is IR-active. Other peaks around  $321\text{cm}^{-1}$ ,  $344\text{cm}^{-1}$ ,  $403\text{cm}^{-1}$ ,  $690\text{cm}^{-1}$  are due to multiple phonon  $A_1$  (TO) and  $E_1$  (TO) scattering processes. These modes are reflecting the strength of polar bonds.

The bands for NiO and Mg-ZnO appeared separately and indicating the formation of mixed metal oxide thin films.<sup>86-88</sup>



**Figure 29: Raman spectra of NiO-(Mg-ZnO)/FTO thin films**

Figure 30 is representing the comparison Raman spectra of pure NiO, pure Mn<sub>2</sub>O<sub>3</sub> and mixed NiO-Mn<sub>2</sub>O<sub>3</sub>/FTO thin films. The bands at 489 cm<sup>-1</sup> and 1098 cm<sup>-1</sup> are as a result of first and second phonon scattering. They are the confirmation of face centered cubic structure of NiO. For pure Mn<sub>2</sub>O<sub>3</sub>, main Raman active bands at 307-312 cm<sup>-1</sup>, 347 cm<sup>-1</sup>, 563 cm<sup>-1</sup>, 655 cm<sup>-1</sup> represents the out of plane (bending modes), asymmetric stretching due to Mn-O-Mn bridge oxygen species and Mn<sub>2</sub>O<sub>3</sub> groups are responsible for (symmetric stretching), respectively. In the composite Raman vibrational peaks for both NiO and Mn<sub>2</sub>O<sub>3</sub> appeared and slight blue shift is observed which may be due to changes in morphology in composite as compared to pure.<sup>89,90</sup>

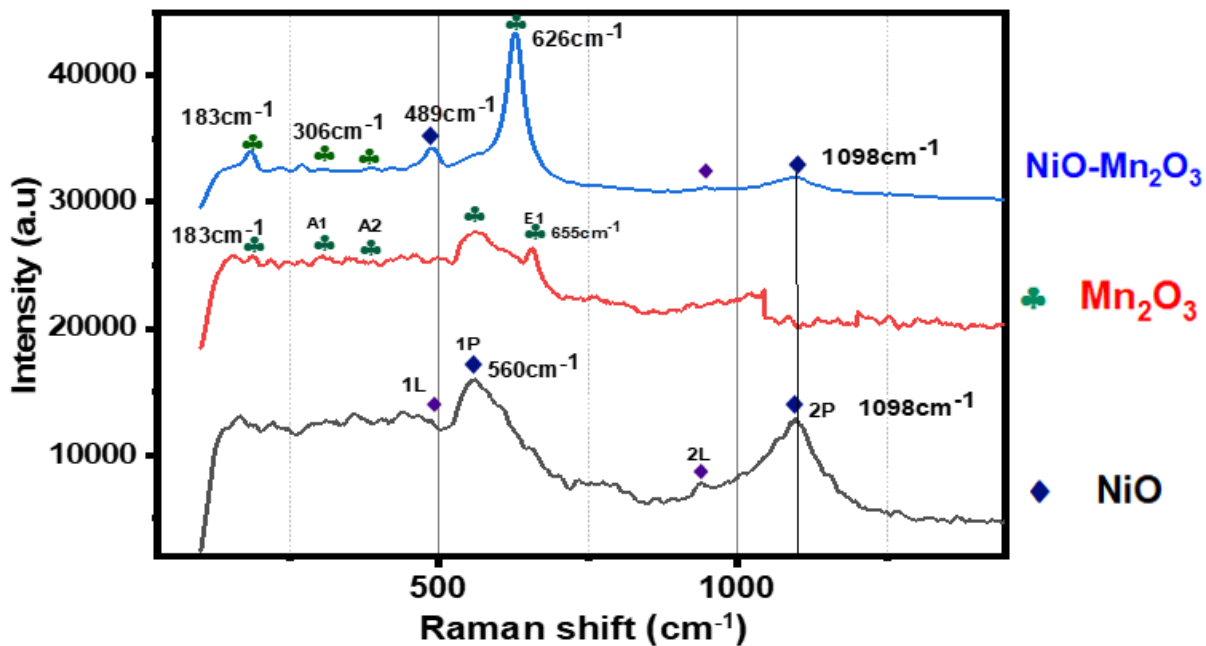


Figure 30: Comparison of Raman spectra of NiO, Mn<sub>2</sub>O<sub>3</sub>, NiO-Mn<sub>2</sub>O<sub>3</sub>/FTO thin films

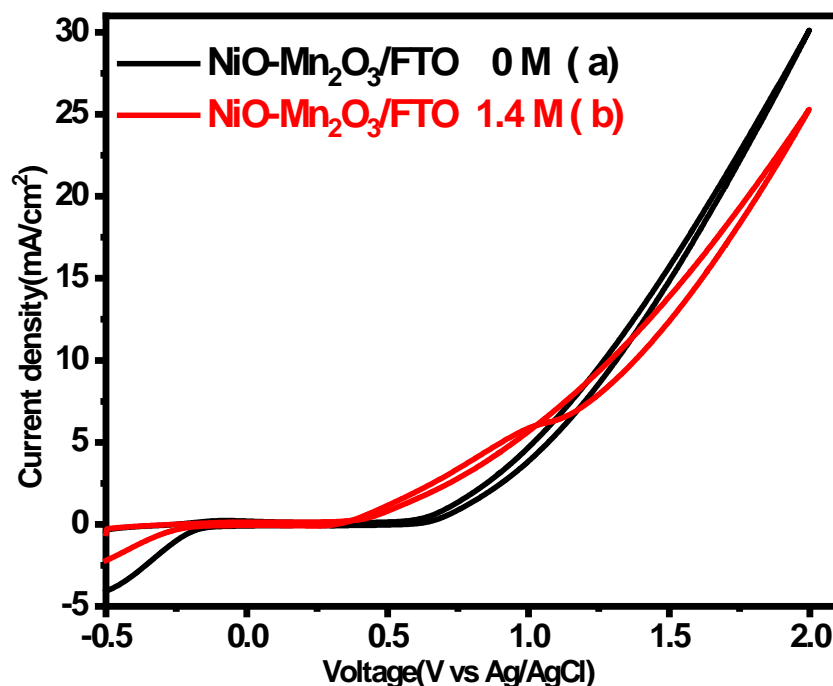
## 4.2 Electrochemical oxidation of Methanol

### Cyclic Voltammetry (CV)

#### 4.2.1.1 Electrocatalytic performance of NiO-Mn<sub>2</sub>O<sub>3</sub>/FTO thin films

The electrocatalytic activity of NiO-Mn<sub>2</sub>O<sub>3</sub>/FTO films for electrooxidation of methanol was measured in 0.5M NaOH electrolyte solution. The Ag/AgCl was used as reference electrode, Pt wire as counter electrode, and fabricated metal oxide thin films were used as working electrode. The Figure 31 is representing the comparison of cyclic voltammogram of as prepared NiO-Mn<sub>2</sub>O<sub>3</sub>/FTO films which were recorded in the absence and presence of methanol (1.4M) in reaction medium. In the absence of methanol, no prominent peak for oxidation is observed. After the addition of about 1.4 M methanol to electrolyte solution peak for oxidation of methanol appeared in anodic half cycle at 0.99V but current density of 3.2 mA/cm<sup>2</sup> is measured at a potential of 0.65V and scan rate of 100mV/s. The onset potential is the point where product is formed. A prominent change in the value of onset potential has been observed in the absence and presence of methanol

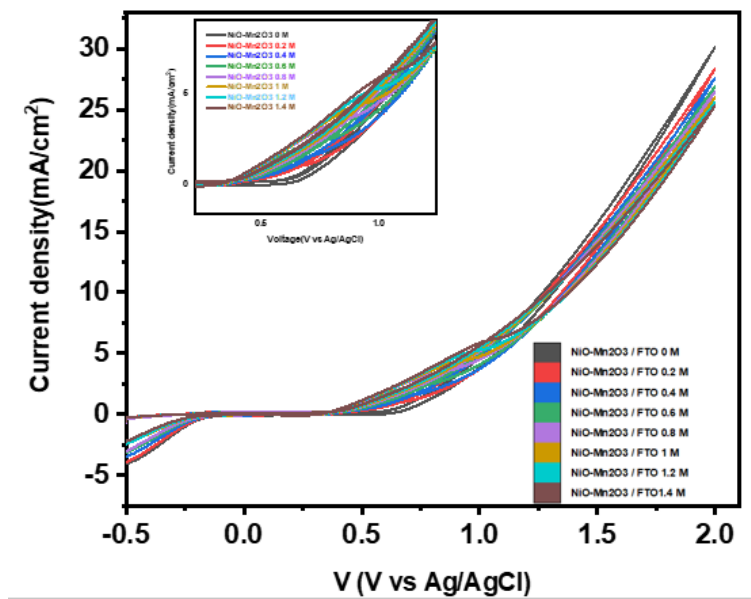
from 0.6 to 0.3V, respectively. During reverse scan an oxidation peak appeared which is indicating that methanol is also oxidized in cathodic half cycle. The reason behind this behavior is that the anodic oxidation peak appeared as a result of chemisorption of methanol in carbonaceous species along with oxidation of  $\text{Ni}^{+2}$ ,  $\text{Ni}^{+3}$  species.<sup>66</sup> Two factors are responsible for decreasing the number of available active sites for methanol oxidation; 1) the oxidation of ( $\text{Ni}^{+2}$  and  $\text{Ni}^{+3}$ ) species, 2) The adsorption of carbonaceous intermediates/products on the working electrode which is referred to as electrode poisoning. As a result of anodic swept in potential the methanol oxidation was observed and attained its maximum current density value that is linked to oxidation of carbonaceous species and active site availability for methanol adsorption.



**Figure 31: Cyclic voltammogram of NiO-Mn<sub>2</sub>O<sub>3</sub>/FTO films in 0.5M NaOH solution at 100 mV/s. a) Without Methanol (0M) b) With Methanol (1.4M)**

It can be seen from the cyclic voltammogram of NiO-Mn<sub>2</sub>O<sub>3</sub>/FTO films that their electrocatalytic activity is dependent on methanol concentration (Figure 32). A steady increase in the current density peak for oxidation of methanol is recorded by increasing the methanol concentration indicating that the current density of all the oxidation peaks is dependent on concentration of

methanol. (Table 5) The process of methanol oxidation is diffusion controlled. Moreover, it is also observed that as methanol concentration was increasing the peaks for its oxidation were shifting towards higher potentials resulted in decreasing the number of available active sites which in turn slowing down the process of oxidation.

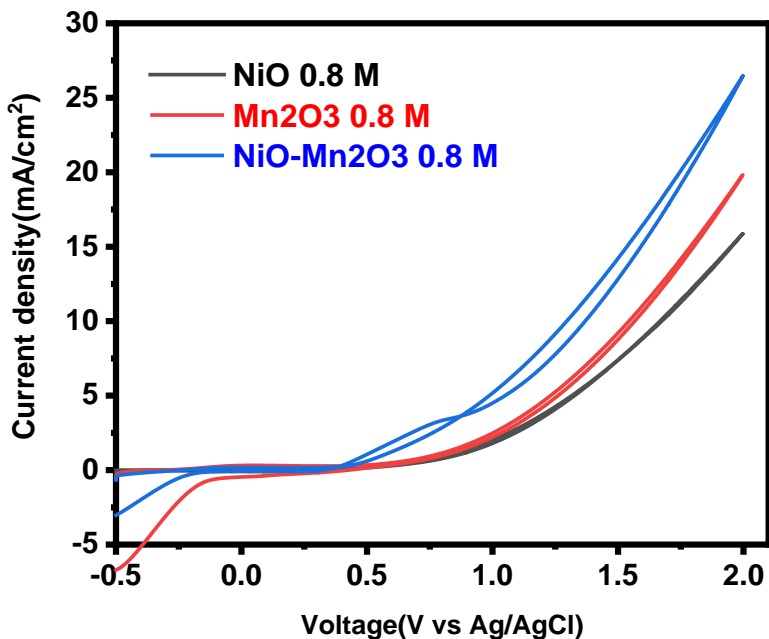


**Figure 32: Cyclic voltammogram of NiO-Mn<sub>2</sub>O<sub>3</sub>/FTO thin films in 0.5M NaOH solution at scan rate of 100mV/s. In the presence of (0, 0.2, 0.4, 0.6, 0.8, 1, 1.2 and 1.4M) methanol solution.**

Sr #	Methanol concentration	Onset Potential (V)	Current density (mA/cm <sup>2</sup> ) at 0.65 V
1	0 M	0.6	0.5
2	0.2 M	0.43	0.9
3	0.4 M	0.41	1.3
4	0.6 M	0.40	2.0
5	0.8 M	0.39	2.35
6	1 M	0.38	2.37
7	1.2M	0.38	2.4
8	1.4M	0.38	2.5

**Table 5: Current densities at 0.65V for various concentrations of Methanol.**

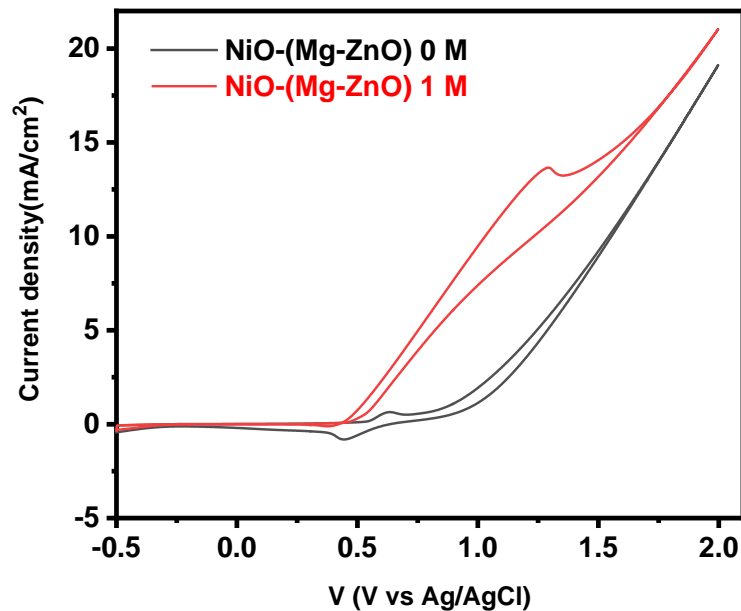
The cyclic voltammograms of pure NiO and Mn<sub>2</sub>O<sub>3</sub> films were also recorded in the absence and presence of different concentration of methanol solution. For comparative analysis, they were compared with cyclic voltammogram of NiO-Mn<sub>2</sub>O<sub>3</sub>/FTO films. The pure NiO and Mn<sub>2</sub>O<sub>3</sub> deposited films showed no prominent peak for oxidation in the presence of 0.8M methanol in 0.5M NaOH solution at scan rate of 100mV/s (Figure 33).



**Figure 33: Cyclic voltammogram of NiO, Mn<sub>2</sub>O<sub>3</sub> and NiO-Mn<sub>2</sub>O<sub>3</sub>/FTO films in 0.5M NaOH and 0.8M methanol solution at 100 mV/s.**

#### **4.2.1.2 Electro-catalytic performance of NiO-(Mg-ZnO)/FTO thin films**

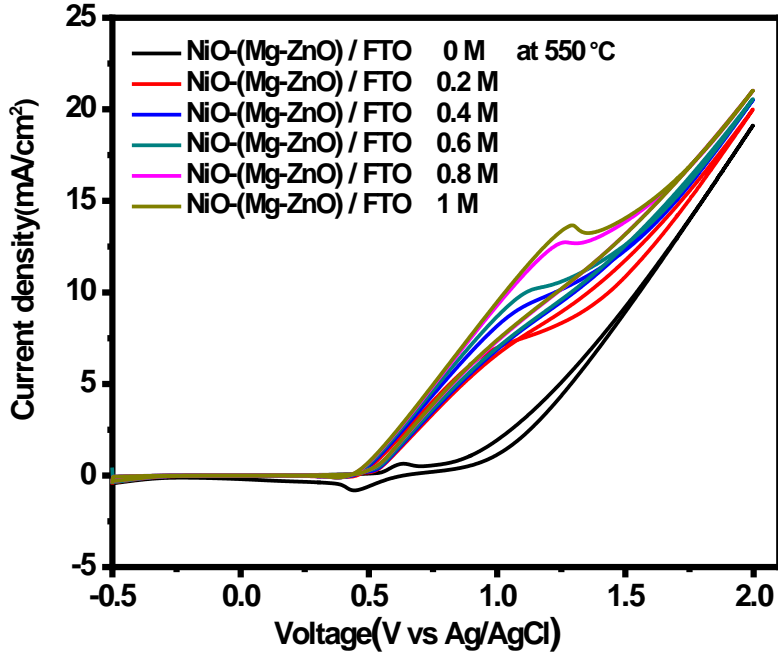
The electrocatalytic activity of NiO-(Mg-ZnO)/FTO films for electrooxidation of methanol was also measured in 0.5M NaOH electrolyte solution. The Ag/AgCl was used as reference electrode, Pt wire as counter electrode, and fabricated metal oxide thin films were used as working electrode. The (Figure 34) is representing the cyclic voltammogram of as prepared NiO-(Mg-ZnO)/FTO films which was recorded in the absence and presence of methanol (1M) solution in reaction medium. In the absence of methanol, the onset potential is 0.8V and at potential of 0.65V the current density value is 0.6mA/cm<sup>2</sup> but in the presence of methanol (1M) solution the onset potential is found at 0.43V and current density of 3.2 mA/cm<sup>2</sup> at 0.65V is measured at scan rate of 100 mV/s. The cyclic voltammogram of same film was recorded three times and gave same results which are the indication of reproducibility and stability of electrode films in alkaline solution.



**Figure 34: Cyclic voltammogram of NiO-(Mg-ZnO)/FTO films in 0.5M NaOH solution at 100 mV/s. a) In absence of methanol b) In the presence of Methanol**

It is evident from the cyclic voltammogram (Figure 35) of NiO-(Mg-ZnO)/FTO films that their electrocatalytic activity is dependent on methanol concentration. A steady increase in the current density peak for oxidation of methanol is recorded by increasing the methanol concentration indicating that the current density of all the oxidation peaks is dependent on concentration of methanol (Table 6). The process of methanol oxidation is diffusion controlled.





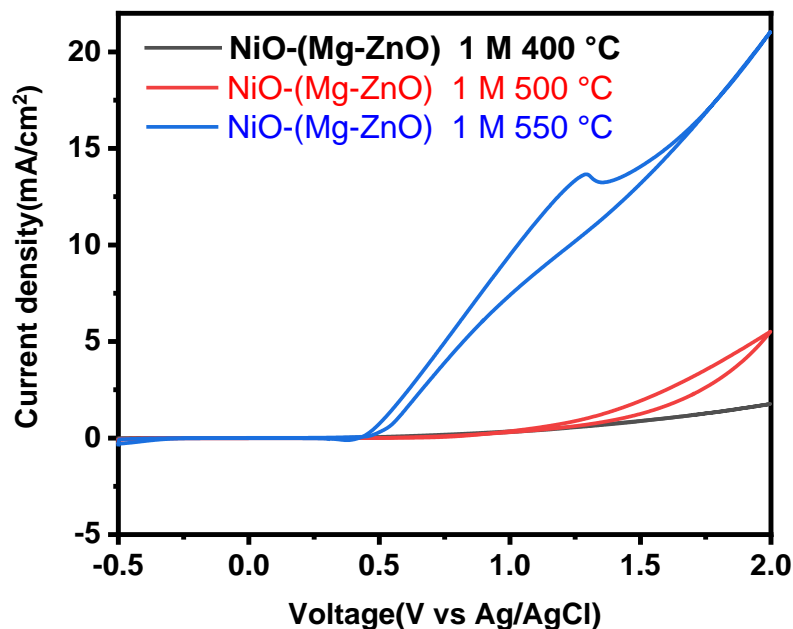
**Figure 35: Cyclic voltammogram of NiO-(Mg-ZnO)/FTO 550°C thin films in 0.5M NaOH solution at scan rate of 100mV/s. In the presence of (0, 0.2, 0.4, 0.6, 0.8, and 1M) methanol.**

Moreover, it is also observed that when methanol concentration was increased the peaks for its oxidation were found to be on higher potentials accordingly that resulted in decreasing the number of available active sites which in turn slows down the process of oxidation.

Sr.#	Methanol concentration	Onset Potential	Current density (mA/cm <sup>2</sup> ) at 0.65V
1	0M (in absence of methanol)	0.8	0.6
2	0.2 M	0.47	2.6
3	0.4 M	0.45	2.8
4	0.6 M	0.44	2.9
5	0.8 M	0.43	3.1
6	1 M	0.43	3.2

**Table 6: Table 5: Current densities at 0.65V for various concentrations of Methanol**

The **NiO-(Mg-ZnO)/FTO** films were prepared at different temperatures (400, 500 and 550°C) by AACVD method and their activity for electrooxidation of methanol was measured. Only the **NiO-(Mg-ZnO)/FTO** films which were fabricated at 550°C were found to be active for electrooxidation of methanol in alkaline medium. Cyclic voltammogram for **NiO-(Mg-ZnO)/FTO** films recorded at different temperature are shown in Figure 36.

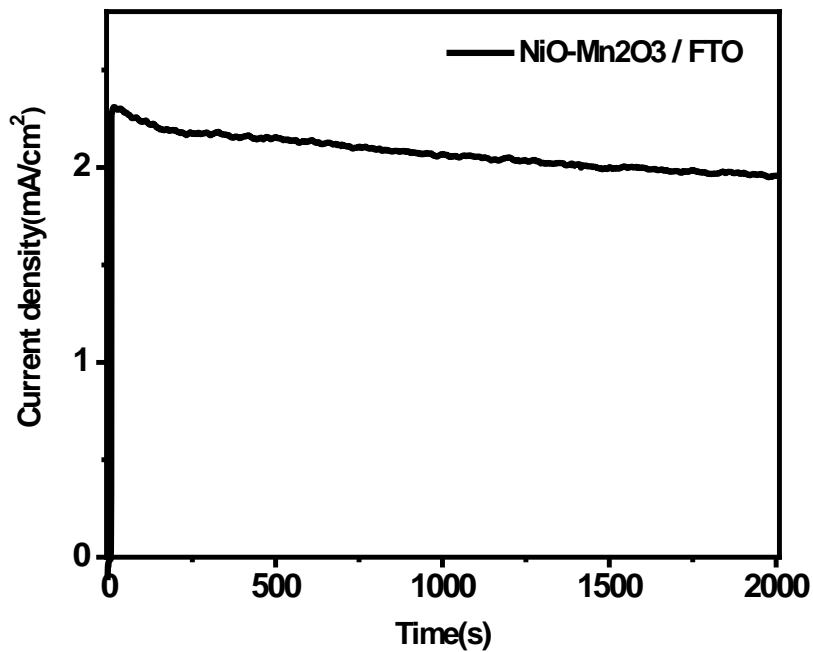


**Figure 36: Comparison of Cyclic voltammogram of NiO-(Mg-ZnO)/FTO films prepared at different temperatures a) 400°C b) 500°C c) 550°C for methanol oxidation in 0.5M NaOH solution at 100mV/s scan rate.**

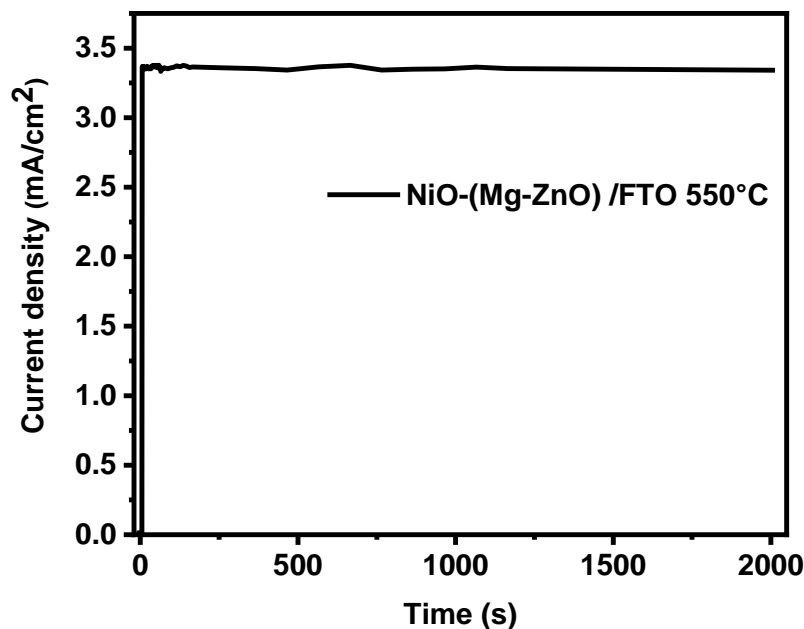
### Chronoamperometry (CA)

Chronoamperometric study was done to evaluate the stabilities of deposited thin films for electrooxidation of methanol. The experiment was done at a potential of 0.6V for 2000s. The synthesized films were taken as working electrode, Ag/AgCl as reference, counter electrode (Pt wire) and NaOH (0.5 M) as electrolyte. The chronoamperometric test of films NiO- Mn<sub>2</sub>O<sub>3</sub>/FTO was done for 2000s, in order to measure their stability towards electrooxidation of Methanol. It can be seen from Figure 37 that NiO- Mn<sub>2</sub>O<sub>3</sub>/FTO films have experienced a current decay of 14% as compared to their current density value at start. The reason behind this current decay is the decreasing concentration of Methanol with passage of time near the surface of electrode. Two factors are responsible for this decrease in methanol concentration, the rapid oxidation of methanol in the beginning and adsorption of reaction intermediates (carbonaceous in nature such as CO) on the electrode's surface thus blocking the active sites and degrading the electrode catalyst. Figure 38 is representing the chronoamperogram of films NiO-(Mg-ZnO)/FTO 550°C which are

synthesized by AACVD method. Under same experimental conditions they have shown stability of 99% after 2000s at potential of 0.6V in the presence of 0.8M methanol.



**Figure 37: Current vs Time plot of NiO- Mn<sub>2</sub>O<sub>3</sub>/FTO films at applied potential of 0.6V, in the presence of 0.5M NaOH solution and 0.8M Methanol.**



**Figure 38: Chronoamperogram of NiO-(Mg-ZnO)/FTO 550°C films at applied potential of 0.6V, in the presence of 0.5M NaOH and 0.8M Methanol.**

### Electrochemical Impedance Spectroscopy (EIS)

Electrocatalytic activity of synthesized catalysts has been evaluated by performing Electrochemical impedance analysis. The experimental parameters include use of Ag/AgCl as reference electrode, Pt wire (Counter electrode), metal oxide films as working electrode in the 0.5M electrolyte NaOH solution and 0.8M Methanol. In the Figure 39 the Nyquist plot of NiO, Mn<sub>2</sub>O<sub>3</sub>, NiO-Mn<sub>2</sub>O<sub>3</sub>/FTO are compared which were recorded in the presence of 0.8M methanol. The semicircle of ceramic films NiO-Mn<sub>2</sub>O<sub>3</sub>/FTO is smaller in diameter with R<sub>ct</sub> value of 71ohm in comparison to pure NiO and Mn<sub>2</sub>O<sub>3</sub> films with R<sub>ct</sub> values 349, 517ohms respectively. It is the synergistic effect between oxides of both metals in combination and the large surface area which are improving the reaction kinetics and thus resulted in decreasing the charge transfer resistance in case of mixed metal oxide. Nyquist plot for NiO-(Mg-ZnO)/FTO 550°C thin films in absence and presence of Methanol recorded and their comparison is shown in Figure 40. The R<sub>ct</sub> value is smaller (571kohm) in methanol presence than in methanol absence (627kohm). It can be stated that methanol addition enhances the reaction kinetics.

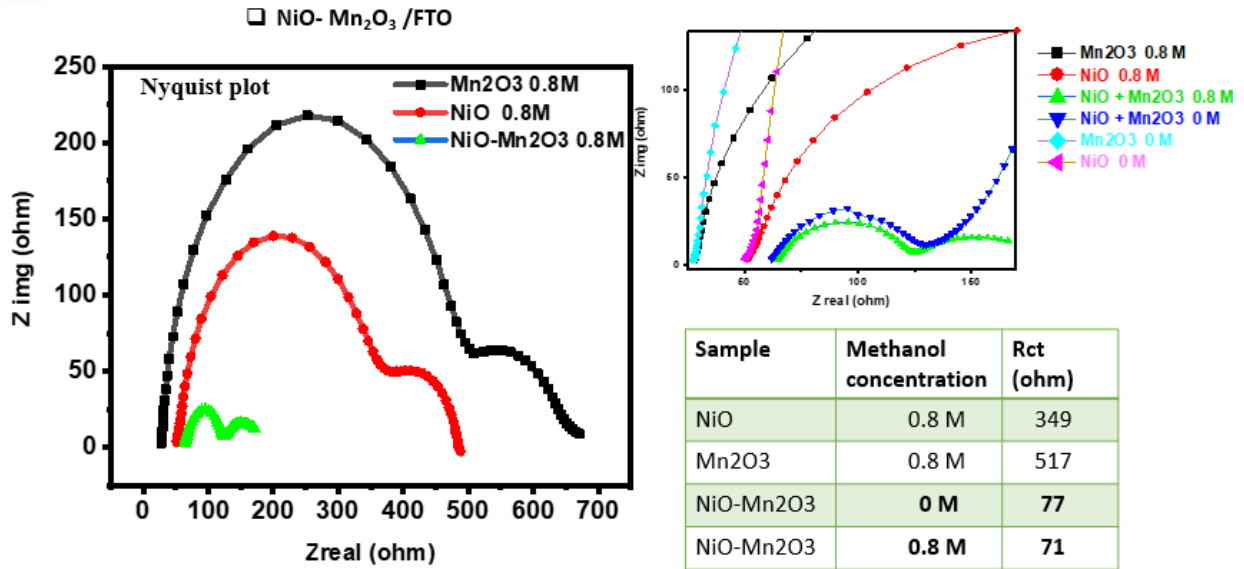


Figure 39: Nyquist plot of Mn<sub>2</sub>O<sub>3</sub>, NiO, NiO-Mn<sub>2</sub>O<sub>3</sub>/FTO thin films in the presence (0.8M) of Methanol.

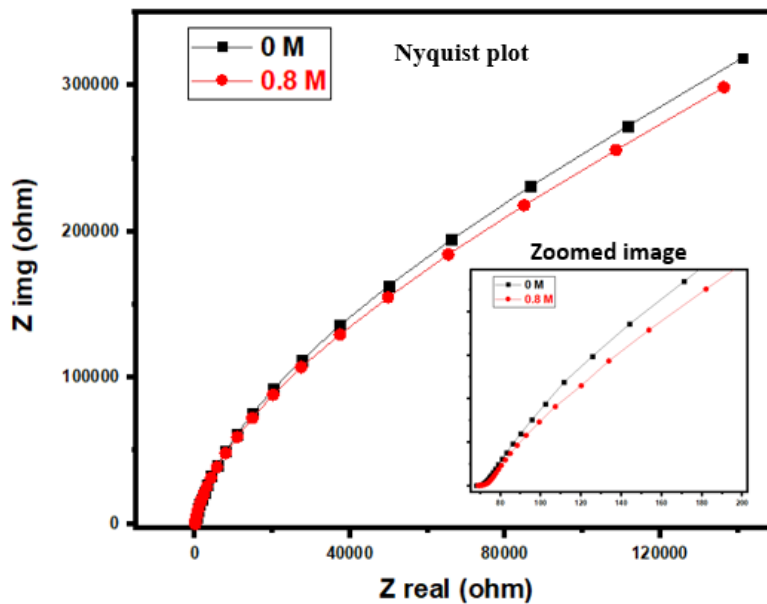


Figure 40: Nyquist plot for NiO-(Mg-ZnO)/FTO 550°C thin films in the absence (0M) and presence (0.8M) of Methanol.

## 5 CHAPTER 05

### CONCLUSION

Direct methanol fuel cells are emerging as a promising clean energy source. They have found applications from portable devices to transport sector. Still their practical applications are restricted due to slow kinetics and methanol crossover. Both anode and cathode electrocatalyst requires modifications. This work is related to synthesis of cheap, pollution free and efficient electrocatalyst for the oxidation of methanol. NiO-(Mg-ZnO)/FTO 550°C thin films are synthesized by AACVD method and NiO/FTO, Mn<sub>2</sub>O<sub>3</sub>/FTO, NiO-Mn<sub>2</sub>O<sub>3</sub>/FTO thin films were fabricated by Dip coating method. Different techniques were used for the characterization of synthesized thin films. Elemental composition was confirmed by EDS analysis and SEM analysis showed that films are uniform and porous. X-ray diffraction and Raman analysis gave information about crystal structure, phase, crystallinity and confirmed the formation of impurity free ceramic thin films. Appearance of peaks separately for metal oxides is the confirmation of mixed metal oxide film formation. Electrocatalytic performance of synthesized films for electro-oxidation of methanol was investigated by use of a three-electrode system based potentiostat in 0.5M electrolyte solution of NaOH by using various electrochemical techniques such as cyclic voltammetry (CV), electrochemical impedance spectroscopy (EIS) and chronoamperometry (CA). NiO-(Mg -ZnO) /FTO thin films fabricated by AACVD method at 550 °C showed better electrochemical activity with current density of 3.2mA/cm<sup>2</sup> vs 0.65 V and maximum value 20.9 mA/ cm<sup>2</sup> in the presence of 1M methanol. The NiO- Mn<sub>2</sub>O<sub>3</sub> /FTO thin films synthesized by Dip coating method showed electrochemical activity with current density 2.35mA/cm<sup>2</sup> vs 0.65 V and maximum of 25.8 mA/ cm<sup>2</sup> in 1.4M methanol. It is the synergistic effect between the metal oxides which is responsible for improved catalytic activity of NiO-(Mg -ZnO) /FTO and NiO- Mn<sub>2</sub>O<sub>3</sub> /FTO thin films. The change in scan rate has direct effect on current densities as transfer of electrons increases or decreases according to change. Chronoamperometric analysis was performed to measure the stability of films. The NiO-(Mg -ZnO) /FTO and NiO- Mn<sub>2</sub>O<sub>3</sub> /FTO thin films showed stabilities of 99% and 86% for 2000s. Small decay in current densities is due to decrease in concentration of methanol with passage of time and formation of intermediates like (CH<sub>3</sub>OH)<sub>ad</sub>, CO<sub>ad</sub>, and CHO<sub>ad</sub> during the electrooxidation of Methanol. EIS studies were also conducted, and they revealed that

in the presence of methanol the charge transfer resistance has decreased. The  $R_{ct}$  value for NiO-(Mg -ZnO) /FTO thin films is 571kohm. For NiO-  $Mn_2O_3$  /FTO thin films  $R_{ct}$  value is  $71\Omega$  which is smaller than the  $R_{ct}$  values for pure NiO and  $Mn_2O_3$  films  $349\Omega$ ,  $517\Omega$ , respectively. The as synthesized ceramic films showed improved catalytic activity, high stability towards oxidation of methanol in basic media in terms of both onset potential and current density. They are proved good candidate to be used as anode catalyst for electro-oxidation of Methanol in Direct Methanol Fuel Cells. Moreover, presence of Methanol decreases the charge transfer resistance and increases the efficiencies of catalytic reaction.



## 6 CHAPTER 06

### REFERENCES

1. Nguyen, K. H. & Kakinaka, M. Renewable energy consumption, carbon emissions, and development stages: Some evidence from panel cointegration analysis. *Renew. Energy* **132**, 1049–1057 (2019).
2. Many, D. Don't Forget Long-Term Fundamental Research in Energy.
3. Mason, J. E. World energy analysis: H2 now or later? *Energy Policy* **35**, 1315–1329 (2007).
4. Durmaz, T. The economics of CCS: Why have CCS technologies not had an international breakthrough? *Renew. Sustain. Energy Rev.* **95**, 328–340 (2018).
5. Moriarty, P. & Honnery, D. A hydrogen standard for future energy accounting? *Int. J. Hydrogen Energy* **35**, 12374–12380 (2010).
6. Gross, M. A planet with two billion cars. *Curr. Biol.* **26**, R307–R310 (2016).
7. Lévy, P. Z., Drossinos, Y. & Thiel, C. The effect of fiscal incentives on market penetration of electric vehicles: A pairwise comparison of total cost of ownership. *Energy Policy* **105**, 524–533 (2017).
8. Martins, F., Felgueiras, C., Smitkova, M. & Caetano, N. Analysis of fossil fuel energy consumption and environmental impacts in european countries. *Energies* **12**, 1–11 (2019).
9. Perera, F. Pollution from fossil-fuel combustion is the leading environmental threat to global pediatric health and equity: Solutions exist. *Int. J. Environ. Res. Public Health* **15**, (2018).
10. Dawood, F., Anda, M. & Shafiullah, G. M. Hydrogen production for energy: An overview. *Int. J. Hydrogen Energy* **45**, 3847–3869 (2020).
11. Abbasi, T. & Abbasi, S. A. Decarbonization of fossil fuels as a strategy to control global

- warming. *Renew. Sustain. Energy Rev.* **15**, 1828–1834 (2011).
12. Rehman, A. & Deyuan, Z. Pakistan’s energy scenario: A forecast of commercial energy consumption and supply from different sources through 2030. *Energy. Sustain. Soc.* **8**, 0–4 (2020).
  13. Shaikh, S. A., Katyara, S. & Khand, Z. Holistic and Scientific Perspectives of Energy Sector in Pakistan : Progression , Challenges and Opportunities. (2020)  
doi:10.1109/ACCESS.2020.3046310.
  14. Fuel cell and its applications - energypedia.
  15. Dazo Water Fuel Technology\_ April 2014.
  16. Batteries, Supercapacitors, and Fuel Cells: Scope. (2007).
  17. WATT. Difference between a battery and a fuel cell - Watt Fuel Cell. (2019).
  18. Sharaf, O. Z. & Orhan, M. F. An overview of fuel cell technology: Fundamentals and applications. *Renew. Sustain. Energy Rev.* **32**, 810–853 (2014).
  19. Carrette, L., Friedrich, K. A. & Stimming, U. Fuel Cells: Principles, Types, Fuels, and Applications. *ChemPhysChem* **1**, 162–193 (2000).
  20. Lai, J. (Jason) & Ellis, M. W. Fuel Cells and Their Applications in Energy Systems. *Power Electron. Renew. Energy Syst. Smart Grid* 443–494 (2019)  
doi:10.1002/9781119515661.ch9.
  21. National Energy Technology Laboratory. Fuel Cell Handbook 7th Edition. *U.S. Dep. Energy* (2000).
  22. Abraham, T. RELIABILITY ANALYSIS OF SOLAR POWERED PEM FUEL CELL PLANT FOR RESIDENTIAL APPLICATION ( With Speclalivation in Industrial Safety and Hazards Management ). **667**,.
  23. Smithsonian Institution. A Basic Overview of Fuel Cell Technology. 4 (2018).
  24. NORIHIRO, O. FUEL CELL | Fuel cell. 2003 (2000).

25. Joghee, P., Malik, J. N., Pylypenko, S. & O'Hayre, R. A review on direct methanol fuel cells – In the perspective of energy and sustainability. *MRS Energy Sustain.* **2**, 1–31 (2015).
26. Riaz, A., Zahedi, G. & Klemeš, J. J. A review of cleaner production methods for the manufacture of methanol. *J. Clean. Prod.* **57**, 19–37 (2013).
27. Guil-López, R. *et al.* Methanol synthesis from CO<sub>2</sub>: A review of the latest developments in heterogeneous catalysis. *Materials (Basel)*. **12**, (2019).
28. Sajgure, M., Kachare, B., Gawhale, P., Waghmare, S. & Jagadale, G. Direct Methanol Fuel Cell: A Review. *Int. J. Curr. Eng. Technol. INPRESSCO IJCET Spec. Issue* **6**, 2277–4106 (2016).
29. Ni, M., Leung, M. K. H. & Leung, D. Y. C. Technological development and prospect of alkaline fuel cells. *16th World Hydrog. Energy Conf. 2006, WHEC 2006* **1**, 842–848 (2006).
30. Rahim, M. A. A., Hameed, R. M. A. & Khalil, M. W. Nickel as a catalyst for the electro-oxidation of methanol in alkaline medium. *J. Power Sources* **134**, 160–169 (2004).
31. citation-229291760.
32. Mahapatra, S. S. & Datta, J. Characterization of Pt-Pd/C Electrocatalyst for Methanol Oxidation in Alkaline Medium. *Int. J. Electrochem.* **2011**, 1–16 (2011).
33. citation-245105135.
34. Spendelow, J. S., Goodpaster, J. D., Kenis, P. J. A. & Wieckowski, A. Methanol Dehydrogenation and Oxidation on Pt(111) in Alkaline Solutions. *Langmuir* **22**, 10457–10464 (2006).
35. Halim, F. A., Hasran, U. A., Masdar, M. S., Kamarudin, S. K. & Daud, W. R. W. Overview on Vapor Feed Direct Methanol Fuel Cell. *APCBEE Procedia* **3**, 40–45 (2012).
36. Qian, W., Wilkinson, D. P., Shen, J., Wang, H. & Zhang, J. Architecture for portable direct liquid fuel cells. *J. Power Sources* **154**, 202–213 (2006).

37. Hacquard, A. Improving and Understanding Direct Methanol Fuel Cell (DMFC) Performance. *PhD Thesis WORCESTER*, 107 (2005).
38. Kamarudin, S. K., Daud, W. R. W., Ho, S. L. & Hasran, U. A. Overview on the challenges and developments of micro-direct methanol fuel cells (DMFC). *J. Power Sources* **163**, 743–754 (2007).
39. Samimi, F. & Rahimpour, M. R. *Direct Methanol Fuel Cell. Methanol: Science and Engineering* (Elsevier B.V., 2018). doi:10.1016/B978-0-444-63903-5.00014-5.
40. Chen, A. & Holt-Hindle, P. Platinum-based nanostructured materials: synthesis, properties, and applications. *Chem. Rev.* **110**, 3767–3804 (2010).
41. Gong, L. *et al.* Recent development of methanol electrooxidation catalysts for direct methanol fuel cell. *J. Energy Chem.* **27**, 1618–1628 (2018).
42. Kloke, A., Von Stetten, F., Zengerle, R. & Kerzenmacher, S. Strategies for the fabrication of porous platinum electrodes. *Adv. Mater.* **23**, 4976–5008 (2011).
43. Luo, C., Xie, H., Wang, Q., Luo, G. & Liu, C. A review of the application and performance of carbon nanotubes in fuel cells. *J. Nanomater.* **2015**, (2015).
44. Yuda, A., Ashok, A. & Kumar, A. A comprehensive and critical review on recent progress in anode catalyst for methanol oxidation reaction. *Catal. Rev. - Sci. Eng.* (2020) doi:10.1080/01614940.2020.1802811.
45. Abegunde, O. O., Akinlabi, E. T., Oladijo, O. P., Akinlabi, S. & Ude, A. U. Overview of thin film deposition techniques. *AIMS Mater. Sci.* **6**, 174–199 (2019).
46. Read, D. T. & Volinsky, A. A. Measurements for Mechanical Reliability of Thin Films. 337–358 (2009) doi:10.1007/978-90-481-2792-4\_16.
47. Antson, J. United States Patent (19). *Geothermics* **14**, 595–599 (1977).
48. Wang, Y. ( 12 ) United States Patent. **2**, (2004).
49. Jilani, A., Abdel-wahab, M. S. & Hammad, A. H. Advance Deposition Techniques for

Thin Film and Coating. *Mod. Technol. Creat. Thin-film Syst. Coatings* (2017)  
doi:10.5772/65702.

50. Mitzel, J., Arena, F., Walter, T., Stefener, M. & Hempelmann, R. Direct methanol fuel cell - Alternative materials and catalyst preparation. *Zeitschrift fur Phys. Chemie* **227**, 497–540 (2013).
51. Scriven, L. E. Physics and Applications of DIP Coating and Spin Coating. *MRS Proc.* **121**, 717–729 (1988).
52. Schneller, T., Waser, R., Kosec, M. & Payne, D. Chemical solution deposition of functional oxide thin films. *Chem. Solut. Depos. Funct. Oxide Thin Film.* **9783211993**, 1–796 (2013).
53. S0022309397001993.
54. Faustini, M., Louis, B., Albouy, P. A., Kueimmel, M. & Grosso, D. Preparation of Sol–Gel Films by Dip-Coating in Extreme Conditions. *J. Phys. Chem. C* **114**, 7637–7645 (2010).
55. Hou, X. & Choy, K. L. Processing and applications of aerosol-assisted chemical vapor deposition. *Chem. Vap. Depos.* **12**, 583–596 (2006).
56. Marchand, P., Hassan, I. A., Parkin, I. P. & Carmalt, C. J. Aerosol-assisted delivery of precursors for chemical vapour deposition: Expanding the scope of CVD for materials fabrication. *Dalt. Trans.* **42**, 9406–9422 (2013).
57. Mat-Teridi, M. A. *et al.* Fabrication of NiO photoelectrodes by aerosol-assisted chemical vapour deposition (AACVD). *Phys. Status Solidi - Rapid Res. Lett.* **8**, 982–986 (2014).
58. Sapti, M. A Textbook on Fundamentals and Applications of Nanotechnology. *Kemamp. Koneksi Mat. (Tinjauan Terhadap Pendekatan Pembelajaran Savi)* **53**, 1689–1699 (2019).
59. Marshall, D. Scanning electron microscope. *PCI-Paint Coatings Ind.* **2016**, 1–3 (2016).
60. Sampathkumar, P. *et al.* Structure, dynamics, evolution, and function of a major scaffold component in the nuclear pore complex. *Structure* **21**, 560–571 (2013).

61. Bunaciu, A. A., Udriștioiu, E. gabriela & Aboul-Enein, H. Y. X-Ray Diffraction: Instrumentation and Applications. *Crit. Rev. Anal. Chem.* **45**, 289–299 (2015).
62. Back, D. M. *Fourier Transform Infrared Analysis of Thin Films. THIN FILMS FOR ADVANCED ELECTRONIC DEVICES: Physics of Thin Films: Advances in Research and Development* vol. 15 (ACADEMIC PRESS, INC, 1991).
63. Chatti, M. *et al.* Intrinsically stable in situ generated electrocatalyst for long-term oxidation of acidic water at up to 80 °C. *Nature Catalysis* vol. 2 (2019).
64. Rusling, J. F. & Suib, S. L. Characterizing Materials with Cyclic Voltammetry. *Adv. Mater.* **6**, 922–930 (1994).
65. Gramy Instruments Inc. Basics of Electrochemical Impedance Spectroscopy Impedance Values. *Appl. Note Rev. 2.0* 1–28 (2014).
66. Danaee, I., Jafarian, M., Forouzandeh, F., Gobal, F. & Mahjani, M. G. Electrocatalytic oxidation of methanol on Ni and NiCu alloy modified glassy carbon electrode. *Int. J. Hydrogen Energy* **33**, 4367–4376 (2008).
67. Hameed, R. M. A. & El-Khatib, K. M. Ni-P and Ni-Cu-P modified carbon catalysts for methanol electro-oxidation in KOH solution. *Int. J. Hydrogen Energy* **35**, 2517–2529 (2010).
68. Qiu, J. D., Wang, G. C., Liang, R. P., Xia, X. H. & Yu, H. W. Controllable deposition of platinum nanoparticles on graphene as an electrocatalyst for direct methanol fuel cells. *J. Phys. Chem. C* **115**, 15639–15645 (2011).
69. Mansoor, M. A. *et al.* Perovskite-structured PbTiO<sub>3</sub> thin films grown from a single-source precursor. *Inorg. Chem.* **52**, 5624–5626 (2013).
70. Gu, Y. *et al.* Synthesis of bimetallic Ni-Cr nano-oxides as catalysts for methanol oxidation in NaOH solution. *J. Nanosci. Nanotechnol.* **15**, 3743–3749 (2015).
71. Hassan, H. B., Hamid, Z. A. & El-Sherif, R. M. Electrooxidation of methanol and ethanol on carbon electrodeposited Ni-MgO nanocomposite. *Cuihua Xuebao/Chinese J. Catal.* **37**,

- 616–627 (2016).
72. Ahmed, S. *et al.* Semiconducting composite oxide Y<sub>2</sub>CuO<sub>4</sub>-5CuO thin films for investigation of photoelectrochemical properties. *Dalt. Trans.* **43**, 8523–8529 (2014).
  73. Mansoor, M. A., Mazhar, M., McKee, V. & Arifin, Z. Mn<sub>2</sub>O<sub>3</sub>-4TiO<sub>2</sub> semiconducting composite thin films for photo-electrochemical water splitting. *Polyhedron* **75**, 135–140 (2014).
  74. Zhang, J. J. *et al.* Hybrid of molybdenum trioxide and carbon as high performance platinum catalyst support for methanol electrooxidation. *Int. J. Hydrogen Energy* **42**, 2045–2053 (2017).
  75. Mansoor, M. A. *et al.* Iron-manganese-titanium (1:1:2) oxide composite thin films for improved photocurrent efficiency. *New J. Chem.* **41**, 7322–7330 (2017).
  76. Mansoor, M. A. *et al.* Cadmium-manganese oxide composite thin films: Synthesis, characterization and photoelectrochemical properties. *Mater. Chem. Phys.* **186**, 286–294 (2017).
  77. Lim, S. P., Pandikumar, A., Huang, N. M. & Lim, H. N. Silver/titania nanocomposite-modified photoelectrodes for photoelectrocatalytic methanol oxidation. *Int. J. Hydrogen Energy* **39**, 14720–14729 (2014).
  78. Hassan, H. B. & Tammam, R. H. Preparation of Ni-metal oxide nanocomposites and their role in enhancing the electro-catalytic activity towards methanol and ethanol. *Solid State Ionics* **320**, 325–338 (2018).
  79. Merati, Z. & Basiri Parsa, J. Enhancement of the catalytic activity of Pt nanoparticles toward methanol electro-oxidation using doped-SnO<sub>2</sub> supporting materials. *Appl. Surf. Sci.* **435**, 535–542 (2018).
  80. Robinson, J. E., Labrador, N. Y., Chen, H., Sartor, B. E. & Esposito, D. V. Silicon Oxide-Encapsulated Platinum Thin Films as Highly Active Electrocatalysts for Carbon Monoxide and Methanol Oxidation. *ACS Catal.* **8**, 11423–11434 (2018).

81. Munawar, K. *et al.* Pyrochlore-structured Y<sub>2</sub>Ti<sub>2</sub>O<sub>7</sub>-2TiO<sub>2</sub> composite thin films for photovoltaic applications. *J. Aust. Ceram. Soc.* **55**, 921–932 (2019).
82. Mansoor, M. A., Lim, S. P., Yusof, F. B. & Ming, H. N. Propitious Escalation in Photocurrent Response from MnZnO<sub>3</sub> Thin Films Using Methanol as Sacrificial Agent. *J. Electron. Mater.* **48**, 4375–4380 (2019).
83. Özdokur, K. V. *et al.* Fabrication of TiO<sub>2</sub>/ZnO/Pt nanocomposite electrode with enhanced electrocatalytic activity for methanol oxidation. *Vacuum* **155**, 242–248 (2018).
84. El-Kemary, M., Nagy, N. & El-Mehasseb, I. Nickel oxide nanoparticles: Synthesis and spectral studies of interactions with glucose. *Mater. Sci. Semicond. Process.* **16**, 1747–1752 (2013).
85. Chhetri, B. P., Parnell, C. M., Wayland, H. & Rangumagar, A. B. Chitosan-Derived NiO-Mn<sub>2</sub>O<sub>3</sub>/C Nanocomposites as Non-Precious Catalysts for Enhanced Oxygen Reduction Reaction. 922–932 (2018) doi:10.1002/slct.201702907.
86. Kutwade, V. V. *et al.* Enhanced photosensing by Mg-doped ZnO hexagonal rods via a feasible chemical route. *J. Mater. Sci. Mater. Electron.* **32**, 6475–6486 (2021).
87. Jiang, Z. Y., Zhu, K. R., Lin, Z. Q., Jin, S. W. & Li, G. Structure and Raman scattering of Mg-doped ZnO nanoparticles prepared by sol-gel method. *Rare Met.* **37**, 881–885 (2018).
88. Akinkuade, S. T., Meyer, W. E. & Nel, J. M. Effects of thermal treatment on structural, optical and electrical properties of NiO thin films. *Phys. B Condens. Matter* **575**, 1–15 (2019).
89. Naeem, R. *et al.* Fabrication of pristine Mn<sub>2</sub>O<sub>3</sub> and Ag-Mn<sub>2</sub>O<sub>3</sub> composite thin films by AACVD for photoelectrochemical water splitting. *Dalt. Trans.* **45**, 14928–14939 (2016).
90. Niu, X. *et al.* Solvothermal synthesis of 1D nanostructured Mn<sub>2</sub>O<sub>3</sub>: effect of Ni<sup>2+</sup> and Co<sup>2+</sup> substitution on the catalytic activity of nanowires. *RSC Adv.* **5**, 66271–66277 (2015).



## **Dedication**

*To my Parents and Sisters.*